Thanks two reviewers for further reviewing our manuscript. We done some changes in this paper according to their comments. We also improved English language in the new version of this paper.

Reply to Report #1.

It appears that the authors has addressed most of my concerns during the initial manuscript review. While the study did not measure size-resolved CCN data which makes it difficult to compare k values derived from side-by-side HTDMA and CCN measurements, it is still the first report about the aerosol CCN properties in a region that was not previously studied. As a result, I recommend the revised manuscript published in the journal Atmospheric Chemistry and Physics.

The other reviewer provided highly detailed comments to further improve the manuscript and the authors have addressed most of them. However, the response table for comment on L267 should be incorporated into the supplementary documents.

Re: Good suggestion, we have added the corresponding table in the supplementary documents.

Reply to Report #2.

For the response to general comment 2: I did not say that there is no connection between HTDMA and CCN measurements. What I suggested is to make a smoother transition from the HTDMA part (4.1 to 4.3.2) to CCN part (4.3.3 and 4.4).

Re: Good suggestion. We done some improvement, such as adding the sentence "It is reasonable to assume that aerosols are internally mixed when estimating N_{CCN} because H-TDMA data showed that this was the case at XT." at beginning of section 4.4.

For the response to specific comments L156 and L164: I suggest the authors also add this information to the main text to help audience better understand your measurements.

Re: Thanks for the suggestion. We have added the corresponding sentences in the manuscript.

For the response to specific comment L181: from the information provided in the main text and this response, what I understand is: Calibration of flow and SS was "conducted before this campaign and the corresponding parameters were applied in the system". Then, "Five SS levels, i.e., 0.07, 0.1, 0.2, 0.4, and 0.8 %, were set in the CCNC". Another SS calibration was done after the campaign and "The calibrated SS used in this paper was from the mean SS of two calibration results". "The corrected SS levels were 0.11, 0.13, 0.22, 0.40, and 0.75 %, respectively". It means that with the five deltT (calculated internally in CCN according to the calibration parameters from first calibration), the actual SS changed from the original values (0.07, 0.1, 0.2, 0.4, and 0.8 %)

before the campaign to 0.15%, 0.16%, 0.24%, 0.4% and 0.7% at the end of the campaign. But this is not what I saw in the calibration curves shown in the response.

This is also why I suggested another "major revisions". I think the authors should clarify this before the manuscript can be considered for final publication.

Re: We are sorry that the response to specific comment L181 confused the reviewer. Actually, the flow and temperature sensors were calibrated before this campaign and their corresponding parameters were used in the system. The SS calibration is different from these calibrations, as SS is related with the temperature gradient (ΔT) in the cloud chamber, not a certain temperature. We didn't change the corresponding parameters to SS although we calibrated it before the campaign. Figure 1 in this reply shows the results of two SS calibrations, suggesting a very limited change of the relationship between SS and ΔT before and after the campaign. This verifies that our CCN counter performed steadily during this campaign.

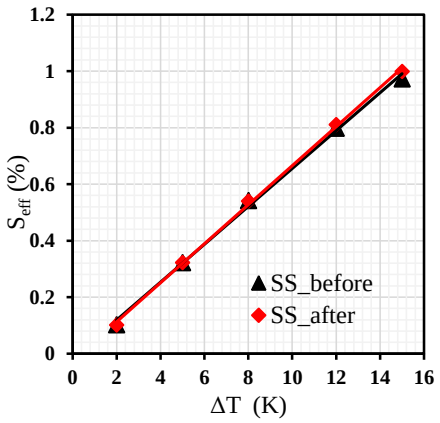

Figure 1. The results of SS calibration experiments with ammonium sulfate: CCN efficiency spectra measured at 5 different temperature gradient (ΔT). SS_before and SS_after are the calibration results before and after the campaign respectively.

For the response to specific comment L183 and L387: with measured PNSD and CCN total number concentration, critical diameter can be calculated as the diameter above which the integration of PNSD equals to the CCN number concentration. This treatment has been used in several studies (e.g. Deng et al., 2013). The advantage is it excludes the influence of the variation of PNSD in the inferred CCN activities, compared with AR.

Re: The reviewer suggests an alternative method to calculate the critical diameter (D_c), so that the corresponding hygroscopicity parameter (κ_{CCN}) can be calculated. However, the shortage of the method lies in that the D_c won't be accurate if the CCN number concentrations (N_{CCN}) have biases. A minor change of D_c will result in a significant change of κ_{CCN} because of the strong sensibility ($\kappa_{CCN} \sim D_c^{-3}$). Figure 2 in this reply shows the κ values from SMPS-CCNc data using the recommended method and HTDMA data in this campaign. It's obvious that κ_{CCN} is larger than κ_{HTDMA}, likely due to the CCNc measurement uncertainties as stated in the manscript. Lower measured N_{CCN} than its actual value in this polluted environment leads to the overestimation of D_c,

then will make a underestimation of κ_{CCN}. This influence is stronger for higher SS (lower D_c) due to higher biases in N_{CCN}, which is also reflected in Fig. 2. In a word, this method maybe not suitable in our data.

Note that our main objective in in L387 is to infer the influence of PBL on the aerosol activation ability. The influence includes the impact of PBL on PNSD, so we think it's appropriate to use AR in this paper.

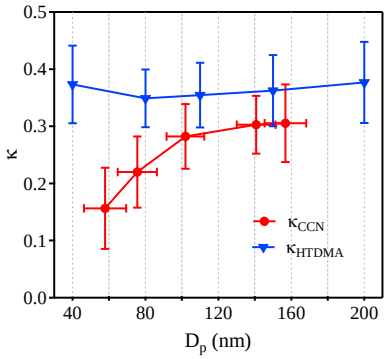

Figure 2. The comparison of hygroscopicity parameter (κ) retrieved from SMPS-CCNc or HTDMA data.

For the response to specific comment L407: I think deleting the sentence will not change the reality that "PM1 composition differ greatly from 40-200 nm particles" as reflected in fig 6.

Re: Yes, it's a good suggestion, we have deleted the corresponding sentence.

For the response to specific comment L434: What I want to point out is, here you can not really prove that 0.31 is a good proxy for the calculation of Nccn. Because as shown in fig. 6, PM1 composition differ greatly from 40-200 nm particles. Probably a kappa of 0.25 or 0.35 can bring similar results just because Nccn is not sensitive on kappa.

Re: Agree, but here we only want to provide a reference value for people who need to calculate the CCN concentration in this region in their models. We have corrected the sentence as "$\kappa = 0.31$ which is a good reference value to model the CCN number concentration in this region".

For the response to specific comment L437: I was not against this statement. I fully agree with it. What I wanted to say is you should not put it in your conclusion since you did not prove it in this section.

Re: Agree. The corresponding sentence about mixing state in the conclusion has been deleted.

Characterization of aerosol hygroscopicity, mixing state, and CCN activity at a suburban site in the central North China Plain

Yuying Wang[1], Zhanqing Li[1], Yingjie Zhang[2], Wei Du[2,3], Fang Zhang[1] , Haobo Tan[4], Hanbing Xu[5], Tianyi Fan[1], Xiaoai Jin[1], Xinxin Fan[1], Zipeng Dong[1], Qiuyan Wang[6], Yele Sun[2,3]

[1]College of Global Change and Earth System Science, Beijing Normal University, Beijing 100875, China

[2]State Key Laboratory of Atmospheric Boundary Layer Physics and Atmospheric Chemistry, Institute of Atmospheric Physics, Chinese Academy of Sciences, Beijing 100029, China

[3]College of Earth Sciences, University of Chinese Academy of Sciences, Beijing 100049, China

[4]Key Laboratory of Regional Numerical Weather Prediction, Institute of Tropical and Marine Meteorology, China Meteorological Administration, Guangzhou 510080, China

[5]Shared Experimental Education Center, Sun Yat-sen University, Guangzhou 510275, China

[6]Collaborative Innovation Center on Forecast and Evaluation of Meteorological Disasters, Nanjing University of Information Science and Technology, Nanjing, 210044, China

*_Correspondence to_: Zhanqing Li (zli@atmos.umd.edu)

带格式的: 字体颜色: 文字 1

带格式的: 字体颜色: 文字 1

带格式的: 字体颜色: 文字 1

Abstract

This study investigates aerosol hygroscopicity, mixing state, and cloud condensation nucleation ~~(CCN) activity~~ as ~~a~~ part of the Atmosphere-Aerosol-Boundary Layer-Cloud ~~(A^{3}BC)~~ Interaction Joint Experiment ~~carried out~~done in the summer of 2016 at Xingtai (XT), a suburban site located in the center of the North China Plain (NCP). In general, the probability density function (PDF) of the hygroscopicity parameter (κ ~~PDF~~) for 40–200 ~~–~~nm particles had a unimodal distribution, and mean κ-PDF patterns for different sizes were similar, suggesting that the particles were highly aged and internally mixed because of strong photochemical reactions. The κ calculated from the hygroscopic growth factor in the daytime and at night~~time~~ ~~showed~~ suggests that photochemical reactions largely enhanced the aerosol hygroscopicity., ~~and the~~This effect became weaker as the particle size increased. In addition, the aerosol hygroscopicity was much larger at XT than ~~those observed~~ at other sites ~~of~~ in the NCP. ~~–~~This is because new particle formation takes place much more frequently in the central NCP, which is heavily polluted from industrial activities, than elsewhere in the region~~for being a center of industrial pollution in China where new particle formation takes place much more frequently than other places~~. The evolution of the planetary boundary layer played a dominant role in dictating aerosol mass concentration. Particle size was the most important factor influencing the ability of aerosols to activate, whereas the effect of chemical composition ~~is~~ was secondary, especially when supersaturation ~~is~~ was high. Using a fixed value of κ = 0.31~~The hygroscopicity parameter of a fixed value (κ = 0.31) is sufficient~~ to calculate the

带格式的: 字体: 非倾斜, 字体颜色: 文字 1

cloud condensation nuclei number concentration~~N_{CCN}~~ in this region suffices.

1. Introduction

Aerosols, defined as the mixture of solid and liquid particles suspended in air, are ubiquitous~~ly present~~ in the atmosphere because of direct emissions from biogenic and anthropogenic sources, and the secondary transformation from gas precursors. Aerosol particles play an important role in climate change~~s~~ through direct and indirect effects (e.g., Ramanathan et al., 2001; ~~Daniel~~ Rosenfeld et al., 2008; Li et al., 2016). However, the impact of aerosols on climate change is difficult to simulate because of the highly variable physical and chemical properties of aerosols, and complex aerosol-cloud interactions (IPCC, 2013; Lebo et al., 2017).

The hygroscopic growth and mixing state of aerosol particles are important for estimating the direct ~~climate~~ radiative effect of aerosols on ~~e~~Earth's climate. This is because the growth and mixing can change the particle size and optical properties of aerosol particles which~~,~~ ~~directly~~ influence~~s~~~~ing~~ the ~~terrestrial~~ solar radiation budget and ~~degrading the~~ atmospheric visibility~~ (e.g. Covert et al., 1972; Stock et al., 2011; Peng et al., 2016; Z. Li et al., 2017a)~~. In addition, aerosol particles can be activated as cloud condensation nuclei (CCN) under supersaturation (SS) conditions. The variability in CCN number concentration (N_{CCN}) can modify both cloud microphysical properties (Twomey, 1974; Albrecht, 1989) and morpho~~no~~logy (Rosenfeld et al., 2008~~; Li et al. 2011~~), and can lead to a broad impact on a wide range of meteorological variables ~~thereby causing an indirect~~ including severe weather events (Li et al., 2017a)~~radiative~~

带格式的: 字体颜色: 文字 1
带格式的: 字体颜色: 文字 1
带格式的: 字体颜色: 文字 1
带格式的: 字体颜色: 文字 1
带格式的: 字体颜色: 文字 1
带格式的: 字体颜色: 文字 1
带格式的: 字体颜色: 文字 1
带格式的: 字体颜色: 文字 1

~~forcing (Twomey, 1974; Albrecht, 1989)~~.

~~–~~Previous studies have addressed three main aerosol properties influencing the CCN activation, namely, particle size, chemical composition, and mixing state. However, their relative importance is different ~~in~~ under different environmental~~s~~ conditions (e.g., Dusek et al., 2006; Ervens et al., 2007; Cubison et al., 2008; Deng et al., 2011; Zhang et al., 2014; Schmale et al., 2018).

Ambient aerosols are composed of different species, including inorganic ions, organic components, black carbon (BC), and mineral dust. Inorganics mainly contain sulfate, nitrate, and ammonium, while organic aerosols (OA) consist of thousands of chemicals (Jacobson et al., 2000). The hygroscopicity and CCN activity of a single component can be characterized according to laboratory studies (e.g., Petters and Kreidenweis, 2007), but the properties of their mixtures are hard to estimate because of the different chemical species and mixing states of particles in the atmosphere. Therefore, aerosol hygroscopicity and CCN activity are very different in different regions due to different chemical compositions. Comprehensive field measurements of aerosol properties in different ~~areas~~ regions are thus necessary to improve models.

China, especially the North China Plain (NCP), has been sufferinged from severe air pollution over the last couple of decades due to rapid industrialization and urbanization~~since its rapid industrialization and urbanization in the last couple of decades.~~, ~~where d~~Diverse sources and aging processes make aerosol properties particularly diverse and complex in this part of the world. As such, the region has drawn much attention ~~in studying~~regarding the aerosol mixing state, hygroscopicity,

带格式的: 字体颜色: 文字 1
带格式的: 字体颜色: 文字 1
带格式的: 字体颜色: 文字 1
带格式的: 字体颜色: 文字 1
带格式的: 字体颜色: 文字 1
带格式的: 字体颜色: 文字 1
带格式的: 字体颜色: 文字 1

and CCN activity (Deng et al., 2011; Liu et al., 2011; Zhang et al., 2014; F. Zhang et al., 2016; S.L. Zhang et al., 2016; Wu et al., 2016; Y. Wang et al., 2017). Liu et al. (2011) and Y. Wang et al. (2017) have suggested that ambient particles are mostly an external mixture with different hygroscopicities. Deng et al. (2011) ~~has~~ have shown that the aerosol number size distribution is critical in the prediction of N_{CCN} while Zhang et al. (2014, 2017) have highlighted the importance of chemical composition in determining particle activation properties. However, ~~all~~ these studies were done using data from the northern part of the NCP. Few studies have focused on the central region of the NCP. Compared to the northern part of the NCP, the central part of the NCP is more affected by industrial emissions ~~where~~ because a dense cluster of China's heavy industries exists there (Fu et al., 2014). Measurements of aerosol properties in the central part of the NCP are thus critically needed to investigate the impact of air pollution on the environment and climate change~~s~~.

Xingtai (XT), a city located in the ~~central area~~center of the NCP, is considered one of the most~~often ranks in the top of~~ polluted cities in China. Local industrial and domestic sources of pollution are the greatest contributors to severe haze events in that region (Wang et al., 2014). A field experiment called the Atmosphere-Aerosol-Boundary Layer-Cloud (A^2BC) Interaction Joint Experiment was ~~carried out~~done at a suburban site in ~~Xingtai~~ XT in the summer of 2016. Differences in aerosol properties at this site and at sites in the northern part of the NCP were found ~~in this study~~.

The paper is organized as follows. Sections 2 and 3 describe the measurement

带格式的: 字体颜色: 文字 1
域代码已更改
带格式的: 字体颜色: 文字 1
域代码已更改
域代码已更改
带格式的: 字体颜色: 文字 1
带格式的: 字体颜色: 文字 1
带格式的: 字体颜色: 文字 1
带格式的: 字体颜色: 文字 1
带格式的: 字体颜色: 文字 1
带格式的: 字体颜色: 文字 1
带格式的: 字体颜色: 文字 1
带格式的: 字体颜色: 文字 1

method and data analysis theory. Section 4 presents and discusses the measurement results, which includes ~~the~~ data time series, aerosol mixing state, hygroscopicity, CCN prediction and its sensitivity to chemical composition. A summary and conclusions are given in section 5.

2. Measurements

2.1. Sampling site and meteorology

The A^{2}BC experiment was ~~carried out~~done at the National Meteorological Basic Station located in XT (37.18°N, 114.37°E, 180 m ~~ASL~~above sea level) from 1 May to 15 June of 2016. This suburban site is situated ~~~~17 km northwest of ~~Xingtai~~ the XT urban area in southern Heibei Province, which is located in the central part of the NCP and to the east of the Taihang Mountains (Fig. 1a). This region is heavily populated, urbanized, and industrialized. ~~The m~~Major industrial manufacturers include coal-based power plants, steel and iron works, glassworks, and cement mills. ~~The w~~Weak diffusion conditions and heavy industrial emissions lead to exceptionally high concentrations of particulate matter (PM) with diameters less than 10 μm ~~(PM_{10})~~ and 2.5 μm ($PM_{2.5}$), as well as gas pollutants such as sulfur dioxide (SO_2), volatile organic compounds (VOCs), and nitrogen oxides (NO_x) during the frequently occurring haze episodes in this region (Wang et al., 2014; Fu et al., 2014). Figure 1b shows the mean distribution of SO_2 concentrations from May of 2012 to 2016~~,~~ which confirms~~ing~~ that the measurement site is located in one of the pollution centers in this region. ~~The~~ A detailed analysis of gas precursors and aerosol chemical species shows that this

带格式的: 字体颜色: 文字 1
带格式的: 字体颜色: 文字 1

station is a ~~good~~ representative site in this region (Zhang et al., 2018).

Time series of meteorological variables measured at this meteorological station are shown in Fig. S1. This site is ~~heavily~~ strongly affected by ~~the~~ mountain-valley winds.~~,~~ Southeasterly winds prevail during the day and at night northwesterly winds prevail~~showing a prevailing southeasterly wind during the day and a northwesterly wind at night~~ (Fig. S1 and Fig. S2). There was almost no precipitation during the study period. The ambient temperature (T) and relative humidity (RH) time series show opposing trends. Campaign-mean values of T and RH are 21.9 °C and 51.6 %, respectively.

2.2. Instrumentation and operation

2.2.1. Aerosol hygroscopicity measurements

The custom-built hygroscopicity tandem differential mobility analyzer (H-TDMA) used in this study has been described in detail by others (Tan et al., 2013; Y. Wang et al., 2017). Briefly, ambient aerosols are first dried and neutralized by a Nafion dryer and a soft X-ray charger. A differential mobility analyzer (DMA_1, model 3081L, TSI Inc.) is used to select monodispersed particles of a certain diameter ~~(D_{p0})~~. The monodisperse~~d~~s particles are then passed through a ~~nafion~~ Nafion humidifier with a controlled higher RH and are humidified. A second DMA (DMA_2, same model as the DMA_1) and a water-based condensation particle counter (WCPC, model 3787, TSI Inc.) are used to measure the number size distribution of the humidified particles. The DMA_1 and WCPC can also be connected directly to measure the 10–400 nm particle

带格式的: 字体颜色: 文字 1

带格式的: 字体颜色: 文字 1

number size distribution (PNSD). In this study, the dry diameters selected by the DMA_1 ~~are~~ were 40, 80, 110, 150, and 200 nm, and ~~,~~t ~~T~~he humidified RH ~~is~~ was set to 85 %~~,~~ ~~the~~ The RH calibration with ammonium sulfate for the H-TDMA is shown in Fig. S3 ~~in the supplement~~.

The hygroscopic growth factor (GF) is defined as the ratio of the humidified diameter at a given RH to the dry diameter:

$$\mathrm{GF} = \frac{D_{\mathrm{p}}(\mathrm{RH})}{D_{\mathrm{p0}}}, \quad (1)$$

where $D_{\mathrm{p}}(\mathrm{RH})$ is the particle diameter at the given RH and D_{p0} is the dry diameter selected by the DMA_1. The measured distribution function versus GF ~~(GF-MDF)~~ can be calculated with WCPC data downstream from the DMA_1 and DMA_2. The GF probability density function ~~(GF-PDF)~~ is then retrieved using the TDMAFIT algorithm (Stolzenburg and McMurry, 1988, 2008).

2.2.2. Aerosol chemical composition measurements

An Aerosol Chemical Speciation Monitor (ACSM) was ~~deployed~~ used to measure ~~the~~ non-refractory submicron aerosol ~~(NR-PM$_1$)~~ species (sulfate, nitrate, ammonium, chloride, and organics) in real-time. A $PM_{2.5}$ URG cyclone (model URG-2000-30ED) was installed in the front of the sampling inlet to remove coarse particles (> 2.5 μm in diameter). Before sampling into the ACSM, aerosol particles were dried (below 40 % RH) by a silica gel diffusion dryer. ~~In addition, t~~The ACSM was calibrated routinely with pure ammonium nitrate to determine its ionization efficiency. More detailed descriptions about the ACSM are given by Ng et al.~~,~~ (2011) and Sun et al.~~,~~ (2012). A

带格式的: 字体颜色: 文字 1
带格式的: 字体颜色: 文字 1
带格式的: 字体颜色: 文字 1
带格式的: 字体颜色: 文字 1
带格式的: 字体颜色: 文字 1
带格式的: 字体颜色: 文字 1
带格式的: 字体颜色: 文字 1
带格式的: 字体颜色: 文字 1
带格式的: 字体颜色: 文字 1
带格式的: 字体颜色: 文字 1
带格式的: 字体颜色: 文字 1
带格式的: 字体颜色: 文字 1
带格式的: 字体颜色: 文字 1
带格式的: 字体颜色: 文字 1
带格式的: 字体颜色: 文字 1
带格式的: 字体颜色: 文字 1

positive matrix factor analysis ~~is~~ was used to analyze the organic spectral matrices according to Ulbrich et al.~~,~~ (2009). Three factors, i.e., hydrocarbon-like OA (HOA), cooking OA (COA), and oxygenated OA (OOA), are chosen as the ACSM dataset. HOA and COA are both primary organic aerosols (POA) while OOA is the secondary organic aerosol (SOA).

The ACSM does not detect refractory material such as BC, so a seven-wavelength aethalometer (AE-33, Magee Scientific Corp.) with a PM with diameters less than 1 μm (PM_1) cyclone was used to measure the BC mass concentration of BC particles with diameters < 1.0 μm ~~(BC-PM_1)~~. Mineral dust and sea salt are the other refractory species, but they typically exist in the coarse mode and contribute negligibly~~make negligible contributions~~ to PM_1 (Juranyi et al., 2010; Meng et al., 2014).

2.2.3. Aerosol size distribution and CCN measurements

The aerosol particle number size distribution (15–685 nm) was measured by a scanning mobility particle sizer (SMPS) that was equipped with a long DMA (model 3081L, TSI Inc.) and a condensation particle counter (~~CPC,~~ model 3775, TSI Inc.). A single-column continuous-flow thermal-gradient cloud condensation nuclei counter (model CCNC-100, DMT Inc.) was ~~applied~~ used to measure the bulk CCN number concentration. Five SS levels, i.e., 0.07, 0.1, 0.2, 0.4, and 0.8–%, were set in the CCNC and the running time was 10 min for each SS level. The SS levels in the CCNC were calibrated with pure ammonium sulfate (Rose et al., 2008) before and after the measurement campaign. The corrected SS levels were 0.11, 0.13, 0.22, 0.40,

带格式的: 字体颜色: 文字 1
带格式的: 字体颜色: 文字 1
带格式的: 字体颜色: 文字 1
带格式的: 非上标/ 下标
带格式的: 字体颜色: 文字 1
域代码已更改
带格式的: 字体颜色: 文字 1
带格式的: 字体颜色: 文字 1
带格式的: 字体颜色: 文字 1
带格式的: 字体颜色: 文字 1

and 0.75-%~~, respectively~~.

The aerosol activation ratio (AR) at a certain SS is calculated as N_{CCN} divided by the total particle number concentration in the 15–685~~-~~nm range ($N_{15–685\ nm}$), i.e., AR = N_{CCN} / $N_{15–685\ nm}$. The SMPS does not measure particle number concentrations below 15 nm. Since the activation critical diameter is always larger than 15 nm at these SS levels (Zhang et al., 2014), this does not affect the calculated N_{CCN}.~~ is not measured by the SMPS, but this does not affect the calculated N_{CCN} because the activation critical diameter is always larger than 15 nm at these SS levels (Zhang et al., 2014).~~ Aerosol particles with diameters ~~larger~~ greater than 685 nm are also not detected by the SMPS. These larger particles will always act as CCN due to their larger dry sizes. ~~However,~~Note that the number concentration above 685 nm in the atmosphere is always negligible (Juranyi et al., 2010).

2.2.4. Other measurements

In this study, a micro-pulse lidar (MPL-4B, Sigmaspace Corp.) was used to study the evolution of the planetary boundary layer (PBL) which plays a crucial role in modulating surface air quality (Z. Li et al., 2017b). The pulse repetition rate of the MPL was 2.5 kHz at a visible wavelength of 532 nm. The peak value of the optical energy of the laser beam was 8 μJ. The pulse duration ranged from 10 to 100 ns, and the pulse interval was set to 200 ns, corresponding to a spatial resolution of 30 m. The MPL-retrieved PBL height is the altitude where a sudden decrease in the scattering coefficient occurs (Brooks, 2003; Quan et al., 2013). Trace gas analyzers

带格式的: 字体颜色: 文字 1
带格式的: 字体颜色: 文字 1
带格式的: 字体颜色: 文字 1
带格式的: 字体颜色: 文字 1
带格式的: 字体颜色: 文字 1
带格式的: 字体颜色: 文字 1
带格式的: 字体颜色: 文字 1
带格式的: 字体颜色: 文字 1

(manufactured by ECOTECH) were used to measure the gaseous species of ozone~~O$_3$~~, SO_2, NO_x, NO, and ~~CO~~carbon monoxide. More detailed descriptions about the analyzers are given by Zhu et al.~~,~~ (2016).

Two containers at ground level housed all sampling instruments. ~~During this campaign, all sampling instruments were placed in two containers at ground level and~~ T~~t~~wo air conditioners ~~were used to~~ maintained the temperature at 20–25-°C inside the containers. All stainless tube inlets were ~~-~~1.5 m above the top of the containers.

3. Theory

3.1. Hygroscopicity parameter

To link hygroscopicity measurements below and above the water vapor saturation, the Köhler theory (Köhler, 1936) is parameterized using the hygroscopicity parameter κ (Petters and Kreidenweis, 2007). This is known as the κ-Köhler theory. According to the theory, the equilibrium equation ~~over~~ for a solution droplet at a saturation ratio $S(D)$ is

$$S(D) = \frac{D^3 - D_d^3}{D^3 - D_d^3(1-\kappa)} \exp\left(\frac{4\sigma_{s/a} M_w}{RT\rho_w D}\right), \quad (2)$$

where D and D_d are the wet and dry droplet diameters, respectively, $\sigma_{s/a}$ is the surface tension coefficient, M_w is the mole mass of water, R is the universal gas constant, T is the temperature, and ρ_w is the density of water.

Below the water vapor saturation, $S(D)$ is RH, D is D_p(RH), and D_d is D_{p0} ~~in~~ from Eq. (1). The κ parameter is then calculated using H-TDMA data according to Eq. (1) and Eq. (2):

$$\kappa_{gf} = (GF^3 - 1) \cdot \left[\frac{1}{RH} \exp\left(\frac{4\sigma_{s/a} M_w}{RT \rho_w D_d GF}\right) - 1\right] \quad . \qquad (3)$$

For a multicomponent particle, the Zdanovskii–Stokes–Robinson (ZSR) mixing rule (Stokes and Robinson, 1966) can also estimate κ using chemical composition data:

$$\kappa_{chem} = \sum_i \varepsilon_i \kappa_i, \qquad (4)$$

where ε_i and κ_i are the volume fraction and ~~κhygroscopicity parameter~~ for the ith chemical component, respectively. The ACSM provides the mass concentrations of inorganic ions and organics. A simplified ion-pairing scheme such as that described by Gysel et al. (2007) is applied to convert ion mass concentrations to mass concentrations of their corresponding inorganic salts (see Table S1 in the supplement). Table S1 also lists κ and the gravimetric density of each individual component under supersaturated conditions. In the following discussions, κ_{gf} and κ_{chem} denote the hygroscopicity parameters derived from H-TDMA measurements and estimated using the ZSR mixing rule, respectively.

3.2. CCN estimation

The critical supersaturation (s_c, s_c = S_c-1) for ~~a dry diameter (~~the D_d~~)~~ of a particle with hygroscopicity κ is calculated from the maximum of the κ-Köhler curve (Eq. 2~~;~~) ~~(~~Petters and Kreidenweis, 2007). The D_d is also the critical diameter corresponding to the s_c when κ is known~~,~~ ~~so~~ Tthe s_c-D_d relationship can thus be established. According to this relationship, the critical diameter ($D_{0,crit}$) can be calculated using the estimated κ_{chem} (Eq. 4) at a given SS. All particles larger than $D_{0,crit}$ will activate as CCN, assuming that aerosols are internally mixed. Then the CCN number

concentration can be estimated from the integral of the aerosol size distribution provided by the SMPS from $D_{0,\mathrm{crit}}$ to the maximum measured size ($D_{\max}$) ~~following Eq. (5)~~:

$$N_{\mathrm{CCN}}(\mathrm{SS}) = \int_{D_{0,\mathrm{crit}}(\mathrm{SS})}^{D_{\max}} \frac{dN(D)}{d\log(D)} d\log(D) \quad . \qquad (5)$$

$N_{\mathrm{CCN}}(\mathrm{SS})$ can then be compared to the number of CCN at the same SS measured by the CCNC ~~(i.e. a closure study)~~.

4. Results and discussion

4.1. Overview

Figures 2 and 3 show ~~the~~ time series of the main aerosol properties measured during the ~~this~~ field campaign. The PNSD changes dramatically (Fig. 2a) and the aerosol number concentration in the 15–50 nm range ($N_{15\text{–}50\ \mathrm{nm}}$) increases sharply in the morning almost every day (Fig. 2b). The time series of the mean diameter (D_{m}) of particles also shows that a growth process occurs after the sharp increase in $N_{15\text{–}50\ \mathrm{nm}}$. All these phenomena suggest that new particle formation (NPF) events ~~occurred~~ frequently occurred at XT during the field experiment (Kulmala et al., 2012; Y. Li et al., 2017). This is likely related to the high concentration of gas precursors ~~mainly~~ from mainly local emissions. High emissions of SO_2 and ~~volatile organic compounds (~~VOCs~~)~~ associated with the high oxidation capacity in a polluted atmosphere make NPF events occur more frequently in northern China (Z. Wang et al., 2017).

Figure 2c-d shows ~~the~~ time series of the probability density functions (PDFs) of κ_{gf} (κ-PDF) for 40-nm and 150-nm particles, respectively. In general, mono-modal

κ-PDFs were observed. This is different from κ-PDFs at other sites in China where bi- and tri-modal distributions ~~are dominant~~dominate (Liu et al., 2011; Ye et al., 2013; Jiang et al., 2016; S. L. Zhang et al., 2016; Y. Wang et al., 2017). Differences in the aerosol mixing state explain this (see section 4.2). ~~This is due to differences in the aerosol mixing state, which will be discussed in section 4.2.~~

Figure 3a shows t~~T~~he bulk mass concentrations of organics, sulfate, nitrate, ammonium, and chloride measured by the ACSM ~~are shown in Fig. 3a, along with~~and the BC mass concentration measured ~~with~~ by the AE-33. Organics and sulfate were the dominant chemical species with mass fractions in PM_1 of 39.1–% and 24.7–%, respectively. Figure 3b-c shows the volume fractions of paired chemical compositions and ~~the hygroscopicity parameter (κ_{chem}) derived from chemical compositions~~, respectively. The average volume fraction of inorganics ($(NH_4)_2SO_4$+NH_4HSO_4+H_2SO_4+NH_4NO_4) was similar to that of organics (POA+SOA), but their volume fractions changed diurnally. In general, the volume fraction of inorganics increased during daytime while the volume fraction of organics decreased. ~~In addition,~~ SOA was the dominant contributor to OA, accounting for ~69-% of the organics volume. This shows that photochemical reactions were strong at XT during the~~is~~ field campaign (Huang et al., 2014). The mean κ_{chem} in Fig. 3c was 0.31 with values ranging from 0.20 to 0.40. The trend in κ_{chem} was similar to that of the volume fraction of inorganics., This suggest~~sing~~ that inorganics played a key role ~~when it comes to~~in κ_{chem}. T~~t~~his is consistent with the study ~~of~~ by Wu et al. (2016).

带格式的: 字体颜色: 文字 1
带格式的: 字体颜色: 文字 1
带格式的: 字体颜色: 文字 1
带格式的: 字体颜色: 文字 1
带格式的: 字体颜色: 文字 1
带格式的: 字体颜色: 文字 1
带格式的: 字体颜色: 文字 1
带格式的: 字体颜色: 文字 1
带格式的: 字体颜色: 文字 1
带格式的: 字体颜色: 文字 1
带格式的: 字体颜色: 文字 1
带格式的: 字体颜色: 文字 1
带格式的: 字体颜色: 文字 1

4.2. Aerosol mixing state and hygroscopicity

~~The average probability density functions of~~ κ_{gf} ~~(~~Figure 4 shows mean κ-PDFs~~)~~ for different particle sizes derived from H-TDMA data ~~are shown in Fig. 4~~. For all particle sizes considered, κ_{gf} ranged from 0 to 0.8, and the κ-PDF patterns were similar. ~~,~~ This suggest~~sing~~ that ~~the~~ hygroscopic compounds in different particle size mode~~s~~ were similar at XT. In general, κ-PDF patterns show only one hydrophilic mode with ~~the~~ a weak hydrophobic mode occasionally appearing at night when photochemical reactions are weak (Fig. S4). The κ-PDF patterns always show bi- or tri-modal distributions~~This is different from what has been reported~~ at other sites in China (Liu et al., 2011; Ye et al., 2013; Jiang et al., 2016; Zhang et al., 2016; Y. Wang et al., 2017)~~, where the κ-PDF patterns always show bi- or tri-modal distributions~~. Based on previous studies (Liu et al., 2011; Y. Wang et al., 2017), ambient aerosols can be classified into three groups according to their κ_{gf} values:

- nearly hydrophobic (NH): $\kappa_{gf} < 0.1$
- less hygroscopic (LH): $0.1 \leqslant \kappa_{gf} < 0.2$
- more hygroscopic (MH): $0.2 \leqslant \kappa_{gf}$

Table 1 gives the number fractions of each group for different particle sizes. The MH group dominated all particle sizes. The number fractions of the NH and LH groups were both less than 6.0 ~~each~~. However, the volume fractions of hydrophobic BC and low-hygroscopic organics (where κ_{BC} is approximately zero and $\kappa_{organic}$ is typically less than 0.1) were ~10.1 % and 47.4 %, respectively, according to chemical composition measurements (Fig. 3b). This suggests that the particles were highly aged

带格式的: 字体颜色: 文字 1

and internally mixed at XT during the~~is~~ field campaign. The c~~C~~oating of sulfates and secondary organics during the aging process changes the structure of BC and makes ~~it~~ these particles grow~~,~~ which can significantly enhance the hygroscopicities~~y~~ of particles (e.g., Zhang et al., 2008; Jimenez et al., 2009; Tritscher et al., 2011; Guo et al., 2016). ~~In addition, t~~The observed unimodal distribution of κ-PDF also suggests the internal mixing state of the particles (Swietlicki et al., 2008).

Figure 5 shows the average size-resolved κ_{gf} derived from H-TDMA data at XT and ~~at~~ other sites in China. At XT, κ_{gf} for different particle sizes were larger in the daytime than at night, and the difference between daytime and nighttime decreased with increasing particle size. This suggests that the impact of photochemical reactions on aerosol hygroscopicity is strong. ~~and that t~~The effect is weaker with increasing particle size because most of the larger particles are always well aged.

The magnitude of κ_{gf} was larger at XT than at other sites ~~of~~ in China. In particular, the magnitude of κ_{gf} was much larger at XT than at sites in the northern part of the NCP, i.e., Beijing, Wuqing, and Xianghe. The lower κ_{gf} in the Beijing urban area ~~of Beijing~~ is likely related to the more severe traffic emissions there (Ye et al., 2013; Wu et al., 2016). Wuqing and Xianghe are located in the suburban area between the two megacities of Beijing and Tianjin and are simultaneously affected by traffic and industrial emissions. ~~–~~The magnitudes of κ_{gf} at these two sites are higher than at Beijing but lower than at XT. Although distant from these megacities, XT is situated in the industrial center of the NCP, so particles there are more internally mixed and highly aged due to the higher concentrations of precursors and strong

带格式的: 字体颜色: 文字 1

photochemical reactions.~~Although XT is located far away from these megacities, it is situated in the industrial center of the NCP, so the higher concentrations of precursors and strong photo-chemical reactions make the particles more internally mixed and highly aged.~~ This is why κ_{gf} ~~in~~ at XT is larger than at other sites. This suggests that the hygroscopicities~~y~~ of particles from different emissions and chemical processes differ in the NCP. ~~In addition, 40~~Forty nm particles were always more hygroscopic than 80-~~-~~nm particles at XT, especially in the daytime.~~,~~ This differed from other sites~~which was also different from other sites. This is~~ likely because the coating effect of sulfates and secondary organics is more significant ~~on~~ for smaller particles (Tritscher et al., 2011; Guo et al., 2016). Furthermore, since the field measurements took place in a locality with heavy industrial activities, it is possible that amine contributed~~s~~ significantly to the hygroscopicity of 40-~~-~~nm particles. Several studies have shown that amine compounds in aerosol phase can be hygroscopic, sometimes at even low RH (e.g.~~,~~ Qiu and Zhang, 2012; Chu et al., 2015; Gomez-Hernandez et al., 2016).

带格式的: 字体颜色: 文字 1
带格式的: 字体颜色: 文字 1
带格式的: 字体颜色: 文字 1

4.3. Diurnal variations in aerosol properties

4.3.1. Diurnal variations in aerosol number and mass concentrations

Figure 6a shows the diurnal variation in MPL-derived PBL height. The PBL height ~~can be determined at~~is the altitude where a sudden decrease in the MPL-measured scattering coefficient occurs ~~from the MPL data~~ (Cohn and Angevine, 2000; Brooks, 2003). Note that the retrieved PBL height is only valid from 07~~:~~00 local

带格式的: 字体颜色: 文字 1
带格式的: 字体颜色: 文字 1

time (LT) to 19:00 LT (Quan et al., 2013). The retrieved PBL height at night is not accurate because of the likely influence of residual aerosols within the nocturnal PBL. The evolution of PBL height from 07:00 LT to 19:00 LT is sufficient to analyze its link with the change in aerosol number and mass concentrations during the daytime. Figure 6b shows diurnal variations in aerosol number and mass concentrations in the 15–685 nm range ($N_{15–685\ nm}$ and $PM_{15–685\ nm}$, respectively). Variations in ~~the~~ $N_{15–685\ nm}$ and $PM_{15–685\ nm}$ trended ~~oppose~~ opposite from each other. From 08:00 LT to 14:00 LT, the PBL height lifted from ~0.5 km to ~0.6 km, while $PM_{15–685\ nm}$ generally decreased from ~24 μg m^{-3} to ~19 μg m^{-3} ~~although there was a slight increase at the beginning of the period~~. This suggests the important effect of PBL evolution on $PM_{15–685\ nm}$. However, $N_{15–685\ nm}$ sharply increased from ~7600 cm^{-3} at 07:00 LT to ~13,000 cm^{-3} at 13:00 LT. This is related to the sudden burst of small Aitken-mode particles (< 50 nm) ~~when~~ during NPF events ~~occurred~~. Newly formed fine particles contribute little to $PM_{15–685\ nm}$. In the evening, $PM_{15–685\ nm}$ increased gradually while $N_{15–685\ nm}$ decreased. ~~This is attributed to t~~The ~~declining trend in~~decline of the nocturnal PBL and particle coagulation and growth explains this. In other words, the evolution of the PBL ~~played a dominant role on~~influenced the aerosol mass concentration, while particle formation and growth had a greater influence on the variation in aerosol number concentration.

4.3.2. Diurnal variation in aerosol hygroscopicity

Figure 6c shows diurnal variations in κ_{gf} and κ_{chem}. Values of κ_{gf} for different particle sizes increased in the morning when the NPF event started. The increase was

带格式的: 字体颜色: 文字 1
带格式的: 字体颜色: 文字 1
带格式的: 字体颜色: 文字 1
带格式的: 缩进: 首行缩进: 0 厘米
带格式的: 字体颜色: 文字 1
带格式的: 字体颜色: 文字 1
带格式的: 字体颜色: 文字 1
带格式的: 字体颜色: 文字 1
带格式的: 字体颜色: 文字 1
带格式的: 字体颜色: 文字 1
带格式的: 字体颜色: 文字 1
带格式的: 字体颜色: 文字 1
带格式的: 字体颜色: 文字 1

sharpest for 40-nm particles.~~All sized κ_{gf} increased beginning from the NPF event, especially for the 40 nm particles.~~ The increase ~~of~~ in κ_{gf} in the morning ~~was~~ synchronized~~ous~~ with the particle number concentration ($N_{15–685\ nm}$) but not with the PBL height, further suggesting the impact of photochemical reactions on aerosol hygroscopicity. The κ_{gf} for 40-nm particles increased from ~0.32 at 07~~:~~00 LT to ~0.44 at 15~~:~~00 LT~~,~~ and approached the κ value of pure ammonium sulfate.~~,~~ This also suggest~~s~~ing that a large amount of hygroscopic compounds were produced during NPF events. Fig. S5 ~~in the supplement~~ shows ~~the~~ sharply increased concentrations of SO_2 and VOCs in the morning and the enhanced atmospheric oxidation capacity under high RH and low *T* conditions. The production of sulfate and SOAs resulted.~~made plenty of sulfate and SOA produced.~~ This is why aerosol hygroscopicity and the occurrence of NPF events increased.~~This is the reason in the increase of aerosol hygroscopicity and the frequent occurrence of NPF events.~~ Zhang et al. (2018) characterized the aerosol chemistry during NPF events in this field campaign.~~Detailed characterization of aerosol chemistry during NPF events in this campaign has been studied in Zhang et al. (2018).~~ The diurnal ~~variation~~ pattern in κ_{gf} for 80–200 nm particles differs from that of 40-nm particles. The differences in κ_{gf} ~~between~~ for 80–200 nm particles in the early morning were large but gradually decreased as the sun rose~~rises~~. ~~After 11:00 LT, t~~The κ_{gf} for 80–200-nm particles were similar but lower than that ~~of~~ for 40-nm particles after 1100 LT. The condensation of sulfates and secondary organics likely caused the enhanced hygroscopicity of the 40–200-nm particles, especially of 40-nm particles (Fig. 6d). ~~All these suggests the~~

带格式的: 字体颜色: 文字 1
带格式的: 字体颜色: 文字 1
带格式的: 字体颜色: 文字 1
带格式的: 字体颜色: 文字 1
带格式的: 字体颜色: 文字 1
带格式的: 字体颜色: 文字 1
带格式的: 字体颜色: 文字 1
带格式的: 字体颜色: 文字 1
带格式的: 字体: 非倾斜, 字体颜色: 文字 1
带格式的: 字体颜色: 文字 1

~~enhanced hygroscopicity in the 40–200 nm particles was likely caused by the condensation of sulfates and secondary organics (Fig. 6d) and the effect was more significant for 40 nm particles.~~

Figure 6c also shows that the κ_{chem} for PM_1 was lower than the κ_{gf} for 40–200~~-~~–nm particles and had a weaker diurnal variation. This feature was stronger at noon when atmospheric oxidation and the aging process were more rapid. The simple ZSR mixing rule is responsible for this.~~The difference was mainly induced by the simple ZSR mixing rule.~~ During the daytime, the condensation of sulfuric acid on organics or BC greatly enhances their hygroscopicities~~y~~ (Zhang et al., 2008; Zhang et al., 2017). The ZSR model cannot accurately represent t~~T~~his phenomenon ~~can't be described accurately by the ZSR model~~. Cruz and Pandis (2000) have shown that the measured κ_{gf} of internally mixed $(NH_4)_2SO_4$-organic aerosols is larger than the predicted κ_{chem} based on the ZSR model.

In summary, the ample supply of ~~effluent~~ SO_2 and VOCs provided sufficient precursors for the strong photochemical reactions at XT during this field campaign, and the productione and condensation of sulfate and SOAs greatly enhanced aerosol hygroscopicity ~~largely~~, especially during the daytime. The oxidation of precursors likely induced the observed frequent NPF events.~~This also suggests that the observed frequent NPF events were mainly induced by the oxidation of precursors.~~

4.3.3. Diurnal variation in CCN number concentration and activation ratio

Figure 7a shows the diurnal variations in N_{CCN} and AR at different SS. In the

带格式的: 字体颜色: 文字 1
带格式的: 字体颜色: 文字 1
带格式的: 字体颜色: 文字 1
带格式的: 字体颜色: 文字 1
带格式的: 字体颜色: 文字 1
带格式的: 字体颜色: 文字 1
带格式的: 字体颜色: 文字 1
带格式的: 字体颜色: 文字 1
带格式的: 字体颜色: 文字 1
域代码已更改
带格式的: 字体颜色: 文字 1
带格式的: 字体颜色: 文字 1
带格式的: 字体颜色: 文字 1
带格式的: 字体颜色: 文字 1
带格式的: 字体颜色: 文字 1
带格式的: 字体颜色: 文字 1
带格式的: 字体颜色: 文字 1

morning, N_{CCN} first decreased then increased while AR showed the opposite trend. This is related to the evolution of the PBL and NPF events. At the initial stage of an NPF event, the newly formed particles were less than 15 nm in size~~,~~ which was below the detection limit of the SMPS. As a result, $N_{15–685\ nm}$ decreased (Fig. 6b) as the PBL lifted~~s~~, and N_{CCN} also decreased. However, the mixing of aged particles within the PBL made the particle size (Fig. 7b) and AR increase slightly. Condensation and the growth of new particles caused the number of fine particles detected by the SMPS to increase rapidly. However, because of their smaller sizes, some of these particles were not activated.~~With condensation and the growth of new particles, the number of fine particles detected by the SMPS increased rapidly but a portion of them cannot be activated because their smaller size.~~ Therefore, N_{CCN} increased, but AR decreased from 08~~:~~00 LT to 14~~:~~00 LT. In the afternoon and evening, N_{CCN} and AR increased slightly ~~with the increase in~~as particle sizes increased (Fig. 7b). ~~However, t~~These trends ~~became weaker~~weakened as SS decreased ~~, this is~~ because the critical diameter is larger at low SS and the influence of aerosol size distribution on N_{CCN} and AR is relatively weaker. ~~This demonstrates that the p~~Particle size was the most important factor influencing ~~the~~ aerosol activation ~~ability~~ and ~~the~~ CCN number concentrations, especially at larger SS ~~levels~~. Figure 6S shows the results from a~~The~~ sensitivity test of particle size in a CCN closure study similar ~~with~~ to that ~~in~~ done by Dusek et al. (2006) ~~was shown in Fig. S6~~.

4.4. CCN estimation from chemical composition data

This section presents a CCN closure study and a discussion of the impact of chemical composition on N_{CCN}. ~~In this section, a CCN closure study is conducted and the impact of chemical composition on N_{CCN} is discussed.~~ It is reasonable to assume that aerosols are internally mixed when estimating N_{CCN} because H-TDMA data showed that this was the case at XT~~HTDMA data has showed particles were highly internally mixed at XT, so the assumption that aerosols are internally mixed when estimating N_{CCN} is reasonable~~. —Figure 8a shows estimated N_{CCN} as a function of measured N_{CCN} using real-time κ_{chem}. The estimated N_{CCN} correlates well with measurements ($R^2 \geqslant 0.85$), but is generally overestimated. The slope of each linearly fitted line is greater than 1.10 and increases with increasing SS. ~~In addition, t~~The relative deviation (RD) increases from 16.2% to 25.2% as SS increases from 0.13% to 0.75—%, suggesting that estimates become worse at larger SS. The large measurement uncertainties of CCNC mainly cause the overestimation of N_{CCN} ~~The overestimation of N_{CCN} is mainly caused by large measurement uncertainties of CCNC~~: (1) T~~t~~he temperature or high flow rates in the CCNC may not allow enough time for particles to reach sizes large enough to be counted by the ~~OPC~~ optical particle counter at the exit of the CCN chamber (Lance et al., 2006; Cubison et al., 2008) and (2) in high particle number concentration environments, water depletion in the CCNC may reduce the counting rate of the CCNC (Deng et al., 2011). These uncertainties make measured N_{CCN} lower than the actual N_{CCN}. At larger SS, ~~those~~ activated aerosols in the cloud chamber of the CCNC are greater in number and smaller in size, so the

带格式的: 字体: 倾斜, 字体颜色: 文字 1
带格式的: 字体颜色: 文字 1, 下标
带格式的: 字体颜色: 文字 1
带格式的: 字体颜色: 文字 1
带格式的: 字体颜色: 文字 1
带格式的: 字体颜色: 文字 1
带格式的: 字体颜色: 文字 1
带格式的: 字体颜色: 文字 1

impact of these uncertainties is greater. Figure S7 shows results from the N_{CCN} closure study for separated N_{CCN}~~The separated N_{CCN} closure study is shown in Fig. S7~~. ~~Figure S7 suggests t~~The CCN closure is ~~very good~~reasonable when N_{CCN} < 5500 cm^{-3}~~,~~ ~~reflecting the validation of the CCN closure method in this study~~.

Figure 8b shows estimated N_{CCN} using the mean value for κ_{chem} (κ_{chem} = 0.31). Compared with results using real-time values for κ_{chem}, the fit parameters and RD change slightly, suggesting that the effect of chemical composition on N_{CCN} is weaker relative to the particle size. Figure 9 shows the sensitivity of estimated N_{CCN} to the variability in chemical composition.~~The sensitivity of estimated N_{CCN} to the variability in chemical composition (κ_{chem}) is further investigated (Fig. 9). In this figure, t~~The variability ~~of~~ in the equipotential lines ~~in~~ of RD suggests that the sensitivity of N_{CCN} is strongly time dependent. This is attributed to the variability of the shape of the aerosol size distribution (Juranyi et al., 2010), which further demonstrates~~, further verifying~~ the importance of particle size to N_{CCN}. The sensitivity of N_{CCN} to chemical composition (κ_{chem}) becomes weaker with increasing SS, suggesting that chemical composition becomes less important in N_{CCN} estimates at larger SS. ~~In addition, the~~ RD is always less than 10~~-~~% when estimating N_{CCN} using the mean value of κ_{chem}~~, suggesting that~~The value κ = 0.31 is thus a good reference value to model ~~the CCN number concentration~~N_{CCN} in this region.~~.~~

In summary, the particle size is the most important factor influencing ~~the~~ aerosol activation~~ ability~~ at XT, especially at larger SS~~ levels~~. The chemical composition was not as important when estimating N_{CCN} because ~~the~~ particles were highly aged and

带格式的: 字体: 倾斜
带格式的: 下标
带格式的: 字体: 倾斜
带格式的: 下标
带格式的: 字体颜色: 文字 1
带格式的: 字体颜色: 文字 1
带格式的: 字体颜色: 文字 1
带格式的: 字体颜色: 文字 1
带格式的: 字体颜色: 文字 1
带格式的: 字体颜色: 文字 1
带格式的: 字体颜色: 文字 1
带格式的: 字体颜色: 文字 1
带格式的: 字体颜色: 文字 1
带格式的: 字体颜色: 文字 1
带格式的: 字体: 倾斜, 字体颜色: 文字 1
带格式的: 字体颜色: 文字 1, 下标
带格式的: 字体颜色: 文字 1
带格式的: 字体颜色: 文字 1
带格式的: 字体颜色: 文字 1
带格式的: 字体颜色: 文字 1
带格式的: 字体颜色: 文字 1
带格式的: 字体颜色: 文字 1
带格式的: 字体颜色: 文字 1
带格式的: 字体颜色: 文字 1
带格式的: 字体颜色: 文字 1
带格式的: 字体颜色: 文字 1
带格式的: 字体颜色: 文字 1
带格式的: 字体: 倾斜, 字体颜色: 文字 1
带格式的: 字体颜色: 文字 1, 下标
带格式的: 字体颜色: 文字 1

internally mixed at XT., ~~aerosol~~ Aerosol hygroscopicity was not sensitive to estimates of N_{CCN}.

5. Summary and conclusions

The Atmosphere-Aerosol-Boundary Layer-Cloud (A^2BC) Interaction Joint Experiment was ~~carried out~~done at a suburban site (Xingtai, or XT) located in the central North China Plain (NCP) from 1 May to 15 June of 2016. The study investigated aerosol hygroscopicity, the mixing state, and CCN activity at ~~the site Xingtai (~~XT~~) were investigated in this study~~.

In general, the probability density function (PDF) of the hygroscopicity parameter κ (κ-PDF) for 40–200 nm particles was a unimodal distribution, which is different from distributions at other sites in China. Particles of all sizes covered a large range of κ_{gf} (the ~~mean~~ hygroscopicity parameter derived from H-TDMA measurements; mostly from 0 to 0.8) and showed similar κ-PDF patterns, suggesting that the hygroscopic compounds in these particles from 40 nm to 200 nm were similar at XT. The κ-PDF patterns also suggest~~s~~ that ~~the~~ particles were highly aged and internally mixed at XT during the ~~this~~ field campaign. This is likely related to strong photochemical reactions.

The mean ~~κ_{gf}~~ for different particle sizes were larger in the daytime than at night. Daytime and nighttime κ_{gf} differences decreased with increasing particle size. ~~This illustrates that t~~The impact of photochemical reactions on aerosol hygroscopicity was strong, and ~~that~~ the effect became weaker as particle size~~s~~ increased~~s~~. The coating

带格式的: 字体: 小四, 非加粗, 字体颜色: 文字 1
带格式的: 字体颜色: 文字 1
带格式的: 字体颜色: 文字 1
带格式的: 字体颜色: 文字 1
带格式的: 字体颜色: 文字 1
带格式的: 字体颜色: 文字 1
带格式的: 字体颜色: 文字 1
带格式的: 字体颜色: 文字 1
带格式的: 字体颜色: 文字 1
带格式的: 字体颜色: 文字 1
带格式的: 字体颜色: 文字 1
带格式的: 字体颜色: 文字 1

of sulfates or secondary organics likely enhanced the hygroscopicities~~y~~ of 40–200-nm particles ~~was likely caused by the coating of sulfates or secondary organics.~~ and ~~t~~This~~e~~ effect was more significant for 40-nm particles. Compared with other sites in China, the aerosol hygroscopicity was much larger at XT because of the sufficient amount of precursors and strong atmospheric oxidation ~~capacity~~. The comparison also shows that the hygroscopicities~~y~~ of particles from different emissions and chemical processes differed ~~largely~~greatly.

New particle formation events occurred frequently at XT during this field campaign. The evolution of the planetary boundary layer ~~(PBL) played a dominant role on~~influenced the aerosol mass concentration, while particle formation and growth had a greater influence on the variation in ~~the~~ aerosol number concentration. Particle size was the most important factor influencing ~~the~~ aerosol activation ~~ability~~ and the CCN number concentration (N_{CCN}) at XT ~~during the field experiment~~, especially at larger supersaturations (SS). Although ~~the~~ estimated N_{CCN} correlate~~d~~s well with measurements ($R^2 \geqslant 0.85$), N_{CCN} was~~is~~ overestimated because of measurement uncertainties. The effect of chemical composition on N_{CCN} ~~is~~ was weaker relative to the particle size. Sensitivity tests show that the impact of chemical composition on N_{CCN} ~~becomes~~ became weaker as SS increase~~d~~s, suggesting that the effect of chemical composition on the estimation of N_{CCN} ~~estimates~~ is less important at larger SS. The value $\kappa = 0.31$ is a good proxy for N_{CCN}~~chemical composition when estimating N_{CCN}~~ ~~use~~for ~~the model at~~in this region ~~XT~~.

~~Our results show that aerosol properties in the middle of the NCP differ from those in~~

带格式的: 字体: 倾斜, 字体颜色: 文字 1

带格式的: 字体颜色: 文字 1, 下标

带格式的: 字体颜色: 文字 1

带格式的: 缩进: 首行缩进: 0 厘米

~~the northern part of the NCP and other regions in China. This is because~~ XT is located in the most polluted region in China. ~~XT is the top most polluted region in China~~ The multitude of factories in the region generates strong emissions~~where there are more plentiful of factories of strong emissionsindustrial emissions in the central NCP~~. The plenitude of gas precursors and strong photochemical reactions at XT make aerosol properties~~, there unique~~there different from those at sites under other polluted conditions~~. More field measurements on gas-particle transformation and aerosol properties in this region are needed~~, which would be meaningful~~ for studying ~~the~~ haze formation mechanisms and climate effects ~~change in the NCP~~.

Data availability. ~~The d~~Data used in the study are available from the first author upon request (wang.yuying@mail.bnu.edu.cn).

Competing interests. The authors declare that they have no conflict of interest.

Author contribution. Z. L. and Y. W. designed the experiment; Y. W., Y. Z., and W. D. carried it out and analyzed the data; other co-authors participated in science discussions and suggested analyses. Y. W. prepared the manuscript with contributions from all co-authors.

Acknowledgements. This work was funded by ~~the~~ National Natural Science Foundation of China (NSFC) research projects (grant no. 91544217, 41675141, 41705125), the National Basic Research Program of China "973" (grant no. 2013CB955801), and the China Scholarship Council (award no. 201706040194). We ~~also~~ thank all participants in the field campaign for their tireless work and cooperation.

References

Albrecht, B. A.: Aerosols, cloud microphysics, and fractional cloudiness, Science, 245, 1227–1230, https://doi.org/10.1126/science.245.4923.1227, 1989.

~~Albrecht B.A.: Aerosols, Cloud Microphysics, and Fractional Cloudiness, Science, 245, 1227-30, 1989.~~

Brooks, I. M.: Finding boundary layer top: application of a wavelet covariance transform to lidar backscatter profiles, J. Atmos. Ocean. Tech., 20, 1092–1105,

带格式的: 字体颜色: 文字 1

带格式的: 字体颜色: 文字 1

带格式的: 字体颜色: 文字 1

带格式的: 行距: 单倍行距

带格式的: 行距: 单倍行距

https://doi.org/10.1175/1520-0426(2003)020<1092:FBLTAO>2.0.CO;2, 2003.
Brooks I.M.: Finding boundary layer top: Application of a wavelet covariance transform to lidar backscatter profiles, J. Atmos. Ocean. Tech., 20, 1092-1105, 2003.
Chu, Y., Sauerwein, M., and Chan, C. K.: Hygroscopic and phase transition properties of alkyl aminium sulfates at low relative humidities, Phys. Chem. Chem. Phys., 17, 19,789–19,796, https://doi.org/10.1039/c5cp02404h, 2015.
Cohn, S. A., and Angevine, W. M.: Boundary layer height and entrainment zone thickness measured by lidars and wind-profiling radars, J. Appl. Meteorol., 39, 1233–1247, https://doi.org/10.1175/1520-0450(2000)039<1233:BLHAEZ>2.0.CO;2, 2000.
Covert, D. S., Charlson, R. J., and Ahlquist, N. C.: A study of the relationship of chemical composition and humidity to light scattering by aerosols, J. Appl. Meteorol., 11, 968–976, https://doi.org/10.1175/1520-0450(1972)011<0968:ASOTRO>2.0.CO;2, 1972.
Cruz, C. N., and Pandis, S. N.: Deliquescence and hygroscopic growth of mixed inorganic–organic atmospheric aerosol, Environ. Sci. Technol., 34, 4313–4319, https://doi.org/10.1021/es9907109, 2000.
Cruz C.N. and Pandis S.N.: Deliquescence and hygroscopic growth of mixed inorganic–organic atmospheric aerosol, Environ. Sci. Technol., 34, 4313-4319, https://doi.org/10.1021/es9907109, 2000.
Cubison, M. J., Ervens, B., Feingold, G., Docherty, K. S., Ulbrich, I. M., Shields, L., Prather, K., Hering, S., and Jimenez, J. L.: The influence of chemical composition and mixing state of Los Angeles urban aerosol on CCN number and cloud properties, Atmos. Chem. Phys., 8, 5649–5667, https://doi.org/10.5194/acp-8-5649-2008, 2008.
Cubison M.J., Ervens B., Feingold G., Docherty K.S., Ulbrich I.M., Shields L., Prather K., Hering S. and Jimenez J.L.: The influence of chemical composition and mixing state of Los Angeles urban aerosol on CCN number and cloud properties, Atmos. Chem. Phys., 8, 5649-5667, https://doi.org/10.5194/acp-8-5649-2008, 2008.
Daniel R., Ulrike L., Raga G.B., O'Dowd C.D., Markku K., Sandro F., Anni R. and Andreae M.O.: Flood or drought: how do aerosols affect precipitation?, Science, 321, 1309-1313, https://doi.org/10.1126/science.1160606, 2008.
Deng, Z. Z., Ma, N., Liu, P. F., Xu, W. Y., Zhao, C. S., Ran, L., Chen, J., Liang, Z., Liang, S., and Huang, M. Y.: Size-resolved and bulk activation properties of aerosols in the North China Plain, Atmos. Chem. Phys., 11, 3835–3846, https://doi.org/10.5194/acp-11-3835-2011, 2011.
Deng Z.Z., Ma N., Liu P.F., Xu W.Y., Zhao C.S., Ran L., Chen J., Liang Z., Liang S. and Huang M.Y.: Size-resolved and bulk activation properties of aerosols in the North China Plain, Atmos. Chem. Phys., 11, 3835-3846, https://doi.org/10.5194/acp-11-3835-2011, 2011.
Dusek, U., Frank, G. P., Hildebrandt, L., Curtius, J., Schneider, J., Walter, S., Chand, D., Drewnick, F., Hings, S., and Jung D.: Size matters more than chemistry for cloud-nucleating ability of aerosol particles, Science, 312, 1375–1378, https://doi.org/10.1126/science.1125261, 2006.
Eichler, H., Cheng, Y. F., Birmili, W., Nowak, A., Wiedensohler, A., Brüggemann, E., Gnauk, T., Herrmann, H., Althausen, D., and Ansmann, A.: Hygroscopic properties and extinction of aerosol particles at ambient relative humidity in South-Eastern

带格式的: 行距: 多倍行距 1.15 字行

带格式的: 行距: 单倍行距

China, Atmos Environ, 42, 6321–6334, https://doi.org/10.1016/j.atmosenv.2008.05.007, 2008.

Ervens, B., Cubison, M., Andrews, E., Feingold, G., Ogren, J. A., Jimenez, J. L., DeCarlo, P., and Nenes, A.: Prediction of cloud condensation nucleus number concentration using measurements of aerosol size distributions and composition and light scattering enhancement due to humidity, J. Geophys. Res.-Atmos., 112, https://doi.org/10.1029/2006JD007426, 2007.

Fu, G. Q., Xu, W. Y., Yang, R. F., Li, J. B., and Zhao, C. S.: The distribution and trends of fog and haze in the North China Plain over the past 30 years, Atmos. Chem. Phys., 14, 11949–11958, https://doi.org/10.5194/acp-14-11949-2014, 2014.

~~Fu G.Q., Xu W.Y., Yang R.F., Li J.B. and Zhao C.S.: The distribution and trends of fog and haze in the North China Plain over the past 30 years, Atmos. Chem. Phys., 14, 11949-11958, https://doi.org/10.5194/acp-14-11949-2014, 2014.~~

Gomez-Hernandez, M., McKeown, M., Secrest, J., Marrero-Ortiz, W., Lavi, A., Rudich, Y., Collins, D. R., and Zhang, R.: Hygroscopic ~~Characteristics~~ characteristics of ~~Alkylaminium~~ alkylaminium ~~Carboxylate~~ carboxylate ~~Aerosols~~aerosols, Environ. Sci. Technol., 50, 2292-2300, https://dx.doi.org/10.1021/acs.est.5b04691, 2016.

Guo, S., Hu, M., Lin, Y., Gomez-Hernandez, M., Zamora, M. L., Peng, J., Collins, D. R., and Zhang, R.: OH-Initiated ~~Oxidation~~ oxidation of m-~~Xylene~~ xylene on ~~Black~~ black ~~Carbon~~ carbon ~~Aging~~aging, Environ. Sci. Technol., 50, 8605–8612, https://dx.doi.org/10.1021/acs.est.6b01272, 2016.

Gysel, M., Crosier, J., Topping, D. O., Whitehead, J. D., Bower, K. N., Cubison, M. J., Williams, P. I., Flynn, M. J., McFiggans, G. B., and Coe, H.: Closure study between chemical composition and hygroscopic growth of aerosol particles during TORCH2, Atmos. Chem. Phys., 7, 6131–6144, https://doi.org/10.5194/acp-7-6131-2007, 2007.

~~Gysel M., Crosier J., Topping D.O., Whitehead J.D., Bower K.N., Cubison M.J., Williams P.I., Flynn M.J., McFiggans G.B. and Coe H.: Closure study between chemical composition and hygroscopic growth of aerosol particles during TORCH2, Atmos. Chem. Phys., 7, 6131-6144, https://doi.org/10.5194/acp-7-6131-2007, 2007.~~

Huang, R., Zhang, Y., Bozzetti, C., Ho, K., Cao, J., Han, Y., Daellenbach, K. R., Slowik, J. G., Platt, S. M., Canonaco, F., Zotter, P., Wolf, R., Pieber, S. M., Bruns, E. A., Crippa, M., Ciarelli, G., Piazzalunga, A., Schwikowski, M., Abbaszade, G., Schnelle-Kreis, J., Zimmermann, R., An, Z., Szidat, S., Baltensperger, U., Haddad, I. E., and Prévôt, A. S. H.: High secondary aerosol contribution to particulate pollution during haze events in China, Nature, 514, 218–222, https://doi.org/10.1038/nature13774, 2014.

~~Huang R., Zhang Y., Bozzetti C., Ho K., Cao J., Han Y., Daellenbach K.R., Slowik J.G., Platt S.M., Canonaco F., Zotter P., Wolf R., Pieber S.M., Bruns E.A., Crippa M., Ciarelli G., Piazzalunga A., Schwikowski M., Abbaszade G., Schnelle-Kreis J., Zimmermann R., An Z., Szidat S., Baltensperger U., Haddad I.E. and Prévôt A.S.H.: High secondary aerosol contribution to particulate pollution during haze events in China, Nature, https://doi.org/10.1038/nature13774, 2014.~~

IPCC: Climate change 2013: Scientific basis, Fifth assessment of the

带格式的: 行距: 单倍行距

带格式的: 行距: 单倍行距

带格式的: 行距: 单倍行距

Inter-governmental Panel on Climate Change, Cambridge University Press, 2013.

Jacobson, M. C., Hansson, H. C., Noone, K. J., and Charlson, R. J.: Organic atmospheric aerosols: review and state of the science, Rev. Geophys., 38, 267–294, https://doi.org/10.1029/1998RG000045, 2000.

~~Jacobson M.C., Hansson H.C., Noone K.J. and Charlson R.J.: Organic atmospheric aerosols: Review and state of the science, Rev. Geophys., 38, 267-294, https://doi.org/10.1029/1998RG000045, 2000.~~

Jiang, R. X., Tan, H. B., Tang, L. L., Cai, M. F., Yin, Y., Li, F., Liu, L., Xu, H. B., Chan, P. W., Deng, X. J., and Wu, D.: Comparison of aerosol hygroscopicity and mixing state between winter and summer seasons in Pearl River Delta region, China, Atmos. Res., 169, 160–170, https://doi.org/10.1016/j.atmosres.2015.09.031, 2016.

~~Jiang R.X., Tan H.B., Tang L.L., Cai M.F., Yin Y., Li F., Liu L., Xu H.B., Chan P.W., Deng X.J. and Wu D.: Comparison of aerosol hygroscopicity and mixing state between winter and summer seasons in Pearl River Delta region, China, Atmos. Res., 169, 160-170, https://doi.org/10.1016/j.atmosres.2015.09.031, 2016.~~

Jimenez, J. L., Canagaratna, M. R., Donahue, N. M., Prevot, A., Zhang, Q., Kroll, J. H., DeCarlo, P. F., Allan, J. D., Coe, H., and Ng, N. L.: Evolution of organic aerosols in the atmosphere, Science, 326, 1525–1529, https://doi.org/10.1126/science.1180353, 2009.

~~Jimenez J.L., Canagaratna M.R., Donahue N.M., Prevot A., Zhang Q., Kroll J.H., DeCarlo P.F., Allan J.D., Coe H. and Ng N.L.: Evolution of organic aerosols in the atmosphere, Science, 326, 1525-1529, https://doi.org/10.1126/science.1180353, 2009.~~

Juranyi, Z., Gysel, M., Weingartner, E., DeCarlo, P. F., Kammermann, L., and Baltensperger, U.: Measured and modelled cloud condensation nuclei number concentration at the high alpine site Jungfraujoch, Atmos. Chem. Phys., 10, 7891–7906, https://doi.org/10.5194/acp-10-7891-2010, 2010.

~~Juranyi Z., Gysel M., Weingartner E., DeCarlo P.F., Kammermann L. and Baltensperger U.: Measured and modelled cloud condensation nuclei number concentration at the high alpine site Jungfraujoch, Atmos. Chem. Phys., 10, 7891-7906, https://doi.org/10.5194/acp-10-7891-2010, 2010.~~

Köhler, H.: The nucleus in and the growth of hygroscopic droplets, T. Faraday Soc., 32, 1152–1161, https://doi.org/10.1039/TF9363201152, 1936.

~~Köhler H.: The nucleus in and the growth of hygroscopic droplets, Transactions of the Faraday Society, 32, 1152-1161, 1936.~~

Kulmala, M., Petäjä, T., Nieminen, T., Sipilä, M., Manninen, H. E., Lehtipalo, K., Dal Maso, M., Aalto, P. P., Junninen, H., and Paasonen, P.: Measurement of the nucleation of atmospheric aerosol particles, Nat. Protoc., 7, 1651–1667, https://doi.org/10.1038/nprot.2012.091, 2012.

~~Kulmala M., Petäjä T., Nieminen T., Sipilä M., Manninen H.E., Lehtipalo K., Dal Maso M., Aalto P.P., Junninen H. and Paasonen P.: Measurement of the nucleation of atmospheric aerosol particles, Nat. Protoc., 7, 1651-1667, https://doi.org/10.1038/nprot.2012.091,2012.~~

Lance, S., Nenes, A., Medina, J., and Smith, J. N.: Mapping the operation of the DMT continuous flow CCN counter, Aerosol Sci. Tech., 40, 242–254, http://dx.doi.org/10.1080/02786820500543290, 2006.

~~Lance S., Nenes A., Medina J. and Smith J.N.: Mapping the operation of the DMT continuous flow CCN counter, Aerosol Sci. Tech., 40, 242-254, http://dx.doi.org/10.1080/02786820500543290,~~

带格式的: 行距: 单倍行距

2006.

Lebo, Z. J., Shipway, B. J., Fan, J., Geresdi, I., Hill, A., Miltenberger, A., Morrison, H., Rosenberg, P., Varble, A., and Xue, L.: Challenges for cloud modeling in the context of aerosol-cloud-precipitation interactions, B. Am. Meteorol. Soc., https://doi.org/10.1175/BAMS-D-16-0291.1, 2017.

Li et al. 2011

Li, Y., Zhang, F., Li, Z., Sun, L., Wang, Z., Li, P., Sun, Y., Ren, J., Wang, Y., Cribb, M., and Yuan, C.: Influences of aerosol physiochemical properties and new particle formation on CCN activity from observation at a suburban site of China, Atmos. Res., 188, 80–89, https://doi.org/10.1016/j.atmosres.2017.01.009, 2017.

Li Y., Zhang F., Li Z., Sun L., Wang Z., Li P., Sun Y., Ren J., Wang Y. and Cribb M.: Influences of aerosol physiochemical properties and new particle formation on CCN activity from observation at a suburban site of China, Atmos. Res., 188, 80-89, https://doi.org/10.1016/j.atmosres.2017.01.009, 2017.

Li, Z., Lau, W. K.-M., Ramanathan, V., Wu, G., Ding, Y., Manoj, M. G., Liu, J., Qian, Y., Li, J., Zhou T., Fan, J., Rosenfeld, D., Ming, Y., Wang, Y., Huang, J., Wang, B., Xu, X., Lee, S.-S., Cribb, M., Zhang, F., Yang, X., Zhao, C., Takemura, T., Wang, K., Xia, X., Yin, Y., Zhang, H., Guo, J., Zhai, P. M., Sugimoto, N., Babu, S. S., and Brasseur, G. P.: Aerosol and monsoon climate interactions over Asia, Rev. Geophys., 54, 866–929, https://doi.org/10.1002/2015RG000500, 2016.

Li Z., Lau W.M., Ramanathan V., Wu G., Ding Y., Manoj M.G., Liu J., Qian Y., Li J. and Zhou T.: Aerosol and monsoon climate interactions over Asia, Rev. Geophys., https://doi.org/10.1002/2015RG000500, 2016.

Li, Z., Daniel, R., and Fan, J. W.: Aerosols and Their their Impact impact on Radiationradiation, Cloudsclouds, Precipitationprecipitation, and Severe severe Weather weather Eventsevents, Oxford Research Encyclopedias: Environmental scienceScience, https://doi.org/10.1093/acrefore/9780199389414.013.126, 2017a.

Li, Z., Li, Z. Guo, J. Guo, A. Ding, a., H. Liao, h., J. Liu, J., Y. Sun, Y., T. Wang, T., H. Xue, H., H. Zhang, H., and B. Zhu, B.2017: Aerosols and boundary-layer interactions and impact on air quality, Natl. Sci. Rev., 4, 810–833, doi:10.1093/nsr/nwx117, 2017b.

Liu, P. F., Zhao, C. S., Bel, T. G., Hallbauer, E., Nowak, A., Ran, L., Xu, W. Y., Deng, Z. Z., Ma, N., Mildenberger, K., Henning, S., Stratmann, F., and Wiedensohler, A.: Hygroscopic properties of aerosol particles at high relative humidity and their diurnal variations in the North China Plain, Atmos. Chem. Phys., 11, 3479–3494, https://doi.org/10.5194/acp-11-3479-2011, 2011.

Liu P.F., Zhao C.S., Bel T.G., Hallbauer E., Nowak A., Ran L., Xu W.Y., Deng Z.Z., Ma N., Mildenberger K., Henning S., Stratmann F. and Wiedensohler A.: Hygroscopic properties of aerosol particles at high relative humidity and their diurnal variations in the North China Plain, Atmos. Chem. Phys., https://doi.org/10.5194/acp-11-3479-2011, 2011.

Lopez-Yglesias, X. F., Yeung, M. C., Dey, S. E., Brechtel, F. J., and Chan, C. K.: Performance Evaluation evaluation of the Brechtel Mfg. Humidified Tandem Differential Mobility Analyzer (BMI HTDMA) for Studying studying Hygroscopic hygroscopic pProperties of aAerosol pParticles, Aerosol Sci. Tech., 48, 969–980,

带格式的: 行距: 单倍行距

带格式的: 行距: 单倍行距

带格式的: 行距: 单倍行距

http://dx.doi.org/10.1080/02786826.2014.952366, 2014.

Meng, J. W., Yeung, M. C., Li, Y. J., Lee, B. Y. L., and Chan, C. K.: Size-resolved cloud condensation nuclei (CCN) activity and closure analysis at the HKUST Supersite in Hong Kong, Atmos. Chem. Phys., 14, 10267–10282, https://doi.org/10.5194/acp-14-10267-2014, 2014.

~~Meng J.W., Yeung M.C., Li Y.J., Lee B.Y.L. and Chan C.K.: Size-resolved cloud condensation nuclei (CCN) activity and closure analysis at the HKUST Supersite in Hong Kong, Atmos. Chem. Phys., 14, 10267-10282, https://doi.org/10.5194/acp-14-10267-2014, 2014.~~

Ng, N. L., Herndon, S. C., Trimborn, A., Canagaratna, M. R., Croteau, P. L., Onasch, T. B., Sueper, D., Worsnop, D. R., Zhang, Q., and Sun, Y. L.: An Aerosol Chemical Speciation Monitor (ACSM) for routine monitoring of the composition and mass concentrations of ambient aerosol, Aerosol Sci. Tech., 45, 780–794, http://dx.doi.org/10.1080/02786826.2011.560211, 2011.~~Ng N.L., Herndon S.C., Trimborn A., Canagaratna M.R., Croteau P.L., Onasch T.B., Sueper D., Worsnop D.R., Zhang Q. and Sun Y.L.: An Aerosol Chemical Speciation Monitor (ACSM) for routine monitoring of the composition and mass concentrations of ambient aerosol, Aerosol Sci. Tech., 45, 780-794, http://dx.doi.org/10.1080/02786826.2011.560211, 2011.~~

~~Peng, J., Hu, M., Guo, S., Du, Z., Zheng, J., Shang, D., Zamora, M. L., Zeng, L., Shao, M., and Wu, Y.: Markedly enhanced absorption and direct radiative forcing of black carbon under polluted urban environments, P. Natl. Acad. Sci. USA, 113, 4266–4271, https://doi.org/10.1073/pnas.1602310113, 2016.~~

~~Peng J., Hu M., Guo S., Du Z., Zheng J., Shang D., Zamora M.L., Zeng L., Shao M. and Wu Y.: Markedly enhanced absorption and direct radiative forcing of black carbon under polluted urban environments, Proceedings of the National Academy of Sciences, 113, 4266-4271, https://doi.org/10.1073/pnas.1602310113, 2016.~~

Petters, M. D., and Kreidenweis, S. M.: A single parameter representation of hygroscopic growth and cloud condensation nucleus activity, Atmos. Chem. Phys., 7, 1961–1971, https://doi.org/10.5194/acp-7-1961-2007, 2007.

~~Petters M.D. and Kreidenweis S.M.: A single parameter representation of hygroscopic growth and cloud condensation nucleus activity, Atmos. Chem. Phys., 7, 1961-1971, https://doi.org/10.5194/acp-7-1961-2007, 2007.~~

Qiu, C., and Zhang, R.: Physiochemical p~~P~~roperties of a~~A~~lkylaminium s~~S~~ulfates: h~~H~~ygroscopicity, t~~T~~hermostability, and d~~D~~ensity, Environ. Sci. Technol., 46, 4474–4480, https://dx.doi.org/10.1021/es3004377, 2012.

Quan, J., Gao, Y., Zhang, Q., Tie, X., Cao, J., Han, S., Meng, J., Chen, P., and Zhao, D.: Evolution of planetary boundary layer under different weather conditions, and its impact on aerosol concentrations, Particuology, 11, 34–40, https://doi.org/10.1016/j.partic.2012.04.005, 2013.

~~Quan J., Gao Y., Zhang Q., Tie X., Cao J., Han S., Meng J., Chen P. and Zhao D.: Evolution of planetary boundary layer under different weather conditions, and its impact on aerosol concentrations, Particuology, 11, 34-40, https://doi.org/10.1016/j.partic.2012.04.005, 2013.~~

Ramanathan, V., Crutzen, P. J., Kiehl, J. T., and Rosenfeld, D.: Aerosols, climate, and the hydrological cycle, Science, 294, 2119–2124,

带格式的: 行距: 单倍行距

带格式的: 行距: 单倍行距

带格式的: 行距: 单倍行距

带格式的: 缩进: 悬挂缩进: 2 字符, 行距: 单倍行距

带格式的: 行距: 单倍行距

https://doi.org/10.1126/science.1064034, 2001.

Rose, D., Gunthe, S. S., Mikhailov, E., Frank, G. P., Dusek, U., Andreae, M. O., and Pöschl, U.: Calibration and measurement uncertainties of a continuous-flow cloud condensation nuclei counter (DMT-CCNC): CCN activation of ammonium sulfate and sodium chloride aerosol particles in theory and experiment, Atmos. Chem. Phys., 8, 1153–1179, https://doi.org/10.5194/acp-8-1153-2008, 2008.

~~Rose D., Gunthe S.S., Mikhailov E., Frank G.P., Dusek U., Andreae M.O. and Pöschl U.: Calibration and measurement uncertainties of a continuous-flow cloud condensation nuclei counter (DMT-CCNC): CCN activation of ammonium sulfate and sodium chloride aerosol particles in theory and experiment, Atmos. Chem. Phys., 8, 1153-1179, https://doi.org/10.5194/acp-8-1153-2008, 2008.~~

Rosenfeld, D., U. Lohmann, G. B. Raga, C. D. O'Dowd, M. Kulmala, S. Fuzzi, A. Reissell, and M. O. Andreae, Flood or drought: How do aerosols affect precipitation?, Science, 321, doi:10.1126/science.1160606, 2008.

Schmale, J., Henning, S., Decesari, S., Henzing, B., Keskinen, H., Sellegri, K., Ovadnevaite, J., Pöhlker, M. L., Brito, J., Bougiatioti, A., Kristensson, A., Kalivitis, N., Stavroulas, I., Carbone, S., Jefferson, A., Park, M., Schlag, P., Iwamoto, Y., Aalto, P., Äijälä, M., Bukowiecki, N., Ehn, M., Frank, G., Fröhlich, R., Frumau, A., Herrmann, E., Herrmann, H., Holzinger, R., Kos, G., Kulmala, M., Mihalopoulos, N., Nenes, A., O'Dowd, C., Petäjä, T., Picard, D., Pöhlker, C., Pöschl, U., Poulain, L., Prévôt, A. S. H., Swietlicki ,E., Andreae, M. O., Artaxo, P., Wiedensohler, A., Ogren, J., Matsuki, A., Yum, S. S., Stratmann, F., Baltensperger, U., and Gysel, M.: Long-term cloud condensation nuclei number concentration, particle number size distribution and chemical composition measurements at regionally representative observatories, Atmos Chem Phys, 18, 2853–2881, https://doi.org/10.5194/acp-18-2853-2018, 2018.

~~Stock, M., Cheng, Y. F., Birmili, W., Massling, A., Wehner, B., Müller, T., Leinert, S., Kalivitis, N., Mihalopoulos, N., and Wiedensohler, A.: Hygroscopic properties of atmospheric aerosol particles over the Eastern Mediterranean: implications for regional direct radiative forcing under clean and polluted conditions, Atmos. Chem. Phys., 11, 4251–4271, https://doi.org/10.5194/acp-11-4251-2011, 2011.~~

Stokes, R. H., and Robinson, R. A.: Interactions in aqueous nonelectrolyte solutions. I. Solute-solvent equilibria, J. Phys. Chem., 70, 2126–2131, https://doi.org/10.1021/j100879a010, 1966.

~~Stokes R.H. and Robinson R.A.: Interactions in aqueous nonelectrolyte solutions. I. Solute-solvent equilibria, The Journal of Physical Chemistry, 70, 2126-2131, 1966.~~

Stolzenburg, M. R., and McMurry, P. H.: Equations governing single and tandem DMA configurations and a new lognormal approximation to the transfer function, Aerosol Sci. Tech., 42, 421–432, http://dx.doi.org/10.1080/02786820802157823, 2008.

Stolzenburg, M. R., and McMurry, P. H.: TDMAFIT user's manual, University of Minnesota, Department of Mechanical Engineering, Particle Technology Laboratory, Minneapolis, 1–61, 1988.

~~Stolzenburg M.R. and McMurry P.H.: TDMAFIT user's manual, University of Minnesota, Department~~

带格式的: 行距: 单倍行距

带格式的: 正文, 左, 缩进: 左侧: 0 厘米, 首行缩进: 0 厘米, 定义网格后不调整右缩进, 不调整西文与中文之间的空格, 不调整中文和数字之间的空格

带格式的: 正文, 左, 缩进: 左侧: 0 厘米, 悬挂缩进: 2 字符, 定义网格后不调整右缩进, 不调整西文与中文之间的空格, 不调整中文和数字之间的空格

带格式的: 行距: 单倍行距

带格式的: 行距: 单倍行距

~~of Mechanical Engineering, Particle Technology Laboratory, Minneapolis, 1-61, 1988.~~

Sun, Y., Wang, Z., Dong, H., Yang, T., Li, J., Pan, X., Chen, P., and Jayne, J. T.: Characterization of summer organic and inorganic aerosols in Beijing, China with an Aerosol Chemical Speciation Monitor, Atmos. Environ., 51, 250–259, https://doi.org/10.1016/j.atmosenv.2012.01.013, 2012.

~~Sun Y., Wang Z., Dong H., Yang T., Li J., Pan X., Chen P. and Jayne J.T.: Characterization of summer organic and inorganic aerosols in Beijing, China with an Aerosol Chemical Speciation Monitor, Atmos. Environ., 51, 250-259, https://doi.org/10.1016/j.atmosenv.2012.01.013, 2012.~~

Swietlicki, E., Hansson, H. C., Hämeri, K., Svenningsson, B., Massling, A., McFiggans, G., McMurry, P. H., Petäjä, T., Tunved, P., Gysel, M., Topping, D., Weingartner, E., Baltensperger, U., Rissler, J., Wiedensohler, A., and Kulmala, M.: Hygroscopic properties of submicrometer atmospheric aerosol particles measured with H-TDMA instruments in various environments—a review, Tellus B, 60, 432–469, https://doi.org/10.1111/j.1600-0889.2008.00350.x, 2008.

~~Swietlicki E., Hansson H.C., HÄMeri K., Svenningsson B., Massling A., McFiggans G., McMurry P.H., PetÄJÄ T., Tunved P., Gysel M., Topping D., Weingartner E., Baltensperger U., Rissler J., Wiedensohler A. and Kulmala M.: Hygroscopic properties of submicrometer atmospheric aerosol particles measured with H-TDMA instruments in various environments—a review, Tellus B, 60, 432-469, https://doi.org/10.1111/j.1600-0889.2008.00350.x, 2008.~~

Tan, H., Xu, H., Wan, Q., Li, F., Deng, X., Chan, P. W., Xia, D., and Yin, Y.: Design and application of an unattended multifunctional H-TDMA system, J. Atmos. Ocean. Tech., 30, 1136–1148, https://doi.org/10.1175/JTECH-D-12-00129.1, 2013.

~~Tan H., Xu H., Wan Q., Li F., Deng X., Chan P.W., Xia D. and Yin Y.: Design and application of an unattended multifunctional H-TDMA system, J. Atmos. Ocean. Tech., 30, 1136-1148, https://doi.org/10.1175/JTECH-D-12-00129.1, 2013.~~

Tritscher, T., Juranyi, Z., Martin, M., Chirico, R., Gysel, M., Heringa, M. F., DeCarlo, P. F., Sierau, B., Prévôt~~Prevot~~, A. S. H., Weingartner, E., and Baltensperger, U.: Changes of hygroscopicity and morphology during ageing of diesel soot, Environ. Res. Lett., 6, https://doi.org/10.1088/1748-9326/6/3/034026, 2011.

Twomey, S.: Pollution and the planetary albedo, Atmos. Environ., 8, 1251–1256, https://doi.org/10.1016/0004-6981(74)90004-3, 1974.

~~Twomey S.: Pollution and the planetary albedo, Atmos. Environ., 8, 1251-1256, 1974.~~

Ulbrich, I. M., Canagaratna, M. R., Zhang, Q., Worsnop, D. R., and Jimenez, J. L.: Interpretation of organic components from Positive Matrix Factorization of aerosol mass spectrometric data, Atmos. Chem. Phys., 9, 2891–2918, https://doi.org/10.5194/acp-9-2891-2009, 2009.

~~Ulbrich I.M., Canagaratna M.R., Zhang Q., Worsnop D.R. and Jimenez J.L.: Interpretation of organic components from Positive Matrix Factorization of aerosol mass spectrometric data, Atmos. Chem. Phys., 9, 2891-2918, https://doi.org/10.5194/acp-9-2891-2009, 2009.~~

Wang, L. T., Wei, Z., Yang, J., Zhang, Y., Zhang, F. F., Su, J., Meng, C. C., and Zhang, Q.: The 2013 severe haze over the southern Hebei, China: model evaluation, source apportionment, and policy implications, Atmos. Chem. Phys. Disc., 13, 3151–3173, https://doi.org/10.5194/acp-14-3151-2014, 2014.

~~Wang L.T., Wei Z., Yang J., Zhang Y., Zhang F.F., Su J., Meng C.C. and Zhang Q.: The 2013 severe~~

带格式的: 行距: 单倍行距

带格式的: 行距: 单倍行距

带格式的: 行距: 单倍行距

带格式的: 行距: 单倍行距

带格式的: 行距: 单倍行距

带格式的: 行距: 单倍行距

haze over southern Hebei, China: model evaluation, source apportionment, and policy implications, Atmos. Chem. Phys., 14, 3151-3173, https://doi.org/10.5194/acp-14-3151-2014, 2014.

Wang, Y., Zhang, F., Li, Z., Tan, H., Xu, H., Ren, J., Zhao, J., Du, W., and Sun, Y.: Enhanced hydrophobicity and volatility of submicron aerosols under severe emission control conditions in Beijing, Atmos. Chem. Phys., 17, 5239–5251, https://doi.org/10.5194/acp-17-5239-2017, 2017.

Wang Y., Zhang F., Li Z., Tan H., Xu H., Ren J., Zhao J., Du W. and Sun Y.: Enhanced hydrophobicity and volatility of submicron aerosols under severe emission control conditions in Beijing, Atmos. Chem. Phys., 17, 5239-5251, https://doi.org/10.5194/acp-17-5239-2017, 2017.

Wang, Z., Wu, Z., Yue, D., Shang, D., Guo, S., Sun, J., Ding, A., Wang, L., Jiang, J., and Guo, H.: New particle formation in China: current knowledge and further directions, Sci. Total Environ., 577, 258–266, https://doi.org/10.1016/j.scitotenv.2016.10.177, 2017.

Wang Z., Wu Z., Yue D., Shang D., Guo S., Sun J., Ding A., Wang L., Jiang J. and Guo H.: New particle formation in China: Current knowledge and further directions, Sci. Total Environ., 577, 258-266, https://doi.org/10.1016/j.scitotenv.2016.10.177, 2017.

Wu, Z. J., Zheng, J., Shang, D. J., Du, Z. F., Wu, Y. S., Zeng, L. M., Wiedensohler, A., and Hu, M.: Particle hygroscopicity and its link to chemical composition in the urban atmosphere of Beijing, China, during summertime, Atmos. Chem. Phys., 16, 1123–1138, https://doi.org/10.5194/acp-16-1123-2016, 2016.

Wu Z.J., Zheng J., Shang D.J., Du Z.F., Wu Y.S., Zeng L.M., Wiedensohler A. and Hu M.: Particle hygroscopicity and its link to chemical composition in the urban atmosphere of Beijing, China, during summertime, Atmos. Chem. Phys., 16, 1123-1138, https://doi.org/10.5194/acp-16-1123-2016, 2016.

Ye, X., Tang, C., Yin, Z., Chen, J., Ma, Z., Kong, L., Yang, X., Gao, W., and Geng, F.: Hygroscopic growth of urban aerosol particles during the 2009 Mirage-Shanghai Campaign, Atmos. Environ., 64, 263–269, https://doi.org/10.1016/j.atmosenv.2012.09.064, 2013.

Ye X., Tang C., Yin Z., Chen J., Ma Z., Kong L., Yang X., Gao W. and Geng F.: Hygroscopic growth of urban aerosol particles during the 2009 Mirage-Shanghai Campaign, Atmos. Environ., 64, 263-269, https://doi.org/10.1016/j.atmosenv.2012.09.064, 2013.

Zhang, F., Li, Y., Li, Z., Sun, L., Li, R., Zhao, C., Wang, P., Sun, Y., Liu, X., Li, J., Li, P., Ren, G., and Fan, T.: Aerosol hygroscopicity and cloud condensation nuclei activity during the AC^{3}Exp campaign: implications for cloud condensation nuclei parameterization, Atmos. Chem. Phys., 14, 13423–13437, https://doi.org/10.5194/acp-14-13423-2014, 2014.

Zhang F., Li Y., Li Z., Sun L., Li R., Zhao C., Wang P., Sun Y., Liu X., Li J., Li P., Ren G. and Fan T.: Aerosol hygroscopicity and cloud condensation nuclei activity during the AC^{3}Exp campaign: implications for cloud condensation nuclei parameterization, Atmos. Chem. Phys., 14, 13423-13437, https://doi.org/10.5194/acp-14-13423-2014, 2014.

Zhang, F., Li, Z., Li, Y., Sun, Y., Wang, Z., Li, P., Sun, L., Wang, P., Cribb, M., Zhao, C., Fan, T., Yang, X., and Wang, Q.: Impacts of organic aerosols and its oxidation level on CCN activity from measurement at a suburban site in China, Atmos. Chem. Phys., 16, 5413–5425, https://doi.org/10.5194/acp-16-5413-2016, 2016.

带格式的: 行距: 单倍行距

带格式的: 行距: 单倍行距

带格式的: 行距: 单倍行距

带格式的: 行距: 单倍行距

带格式的: 行距: 单倍行距

带格式的: 行距: 单倍行距

~~Zhang F., Li Z., Li Y., Sun Y., Wang Z., Li P., Sun L., Wang P., Cribb M., Zhao C., Fan T., Yang X. and Wang Q.: Impacts of organic aerosols and its oxidation level on CCN activity from measurement at a suburban site in China, Atmos. Chem. Phys., 16, 5413-5425, https://doi.org/10.5194/acp-16-5413-2016, 2016.~~

Zhang, F., Wang, Y., Peng, J., Ren, J., Collins, D., Zhang, R., Sun, Y., Yang, X., and Li, Z.: Uncertainty in predicting CCN activity of aged and primary aerosols, J. Geophys. Res.-Atmos., 122, https://doi.org/10.1002/2017JD027058, 2017.

Zhang, R., Khalizov, A. F., Pagels, J., Zhang, D., Xue, H., and McMurry, P. H.: Variability in morphology, hygroscopicity, and optical properties of soot aerosols during atmospheric processing, P. Natl. Acad. Sci. USA, 105, 10291–10296, https://doi.org/10.1073/pnas.0804860105, 2008.

~~Zhang, R., Wang, L., Khalizov, A. F., Zhao, J., Zheng, J., McGraw, R. L., and Molina, L. T.: Formation of nanoparticles of blue haze enhanced by anthropogenic pollution, P. Natl. Acad. Sci. USA, 106, 17650-17654, https://doi.org/10.1073/pnas.0910125106, 2009.~~

Zhang, S. L., Ma, N., Kecorius, S., Wang, P. C., Hu, M., Wang, Z. B., Größ, J., Wu, Z. J., and Wiedensohler, A.: Mixing state of atmospheric particles over the North China Plain, Atmos. Environ., 125, Part A, 152–164, https://doi.org/10.1016/j.atmosenv.2015.10.053, 2016.

Zhang, Y., Du, W., Wang, Y., Wang, Q., Wang, H., Zheng, H., Zhang, F., Shi, H., Bian, Y., Han, Y., Fu, P., Canonaco, F., Prévôt, A. S. H., Zhu, T., Wang, P., Li, Z., and Sun, Y.: Aerosol chemistry and particle growth events at an urban downwind site in the North China Plain, Atmos. Chem. Phys. Discuss., 2018, 1–29, https://doi.org/10.5194/acp-2017-889, 2018.

~~Zhang R., Khalizov A.F., Pagels J., Zhang D., Xue H. and McMurry P.H.: Variability in morphology, hygroscopicity, and optical properties of soot aerosols during atmospheric processing, Proceedings of the National Academy of Sciences, 105, 10291-10296, https://doi.org/10.1073/pnas.0804860105,2008.~~

~~Zhang R., Wang L., Khalizov A.F., Zhao J., Zheng J., McGraw R.L. and Molina L.T.: Formation of nanoparticles of blue haze enhanced by anthropogenic pollution, Proceedings of the National Academy of Sciences, 106, 17650-17654, https://doi.org/10.1073/pnas.0910125106, 2009.~~

~~Zhang S.L., Ma N., Kecorius S., Wang P.C., Hu M., Wang Z.B., Größ J., Wu Z.J. and Wiedensohler A.: Mixing state of atmospheric particles over the North China Plain, Atmos. Environ., 125, Part A, 152-164, https://doi.org/10.1016/j.atmosenv.2015.10.053, 2016.~~

Zhu, Y., Zhang, J., Wang, J., Chen, W., Han, Y., Ye, C., Li, Y., Liu, J., Zeng, L., Wu, Y., Wang, X., Wang, W., Chen, J., and Zhu, T.: Distribution and sources of air pollutants in the North China Plain based on on-road mobile measurements, Atmos. Chem. Phys., 16, 12551–12565, https://doi.org/10.5194/acp-16-12551-2016, 2016.

~~Zhu Y., Zhang J., Wang J., Chen W., Han Y., Ye C., Li Y., Liu J., Zeng L., Wu Y., Wang X., Wang W., Chen J. and Zhu T.: Distribution and sources of air pollutants in the North China Plain based on on-road mobile measurements, Atmos. Chem. Phys., 16, 12551-12565, https://doi.org/10.5194/acp-16-12551-2016, 2016.~~

带格式的: 行距: 单倍行距

带格式的: 行距: 单倍行距

带格式的: 字体颜色: 文字 1

Table 1. ~~The n~~Number fractions of different hygroscopic groups for different particle sizes.

	40 nm	80 nm	110 nm	150 nm	200 nm
NH	5.1 %	5.0 %	5.1 %	5.0 %	5.7 %
LH	4.8 %	4.2 %	4.3 %	4.7 %	5.1 %
MH	90.1 %	90.8 %	90.6 %	90.3 %	89.2 %

NH: nearly hydrophobic; LH: less hygroscopic; MH: more hygroscopic

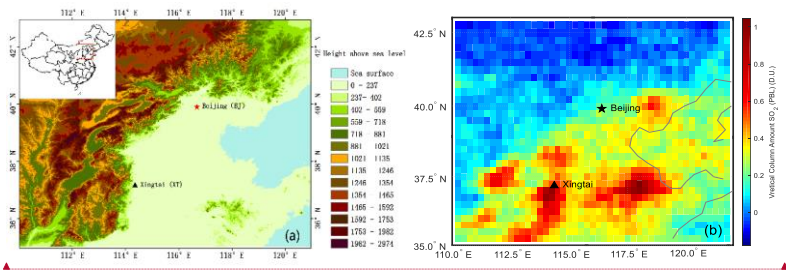

Figure 3. (**a**) Map showing the location of the sampling site and (**b**) the distribution of mean SO_2 concentrations ~~of~~ from May ~~from~~ of 2012 to 2016.

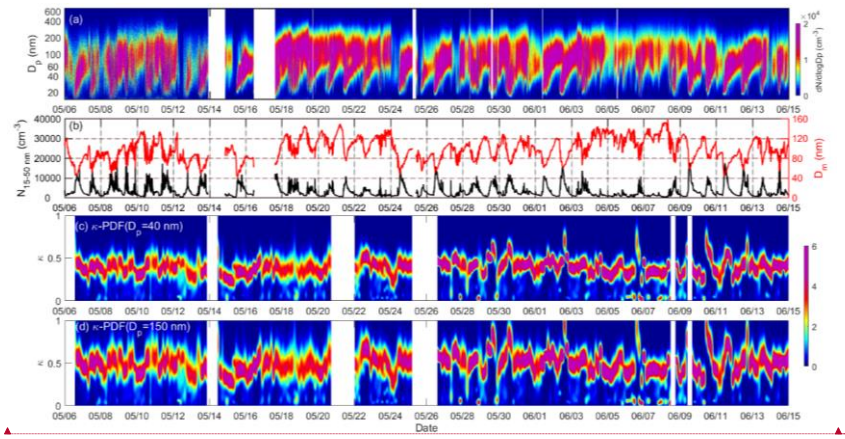

Figure 4. The time series of (**a**) the particle number size distribution ~~(PNSD)~~, (**b**) the aerosol number concentration in the 15–50 nm range ($N_{15–50\ nm}$) and the geometric mean diameter (D_m), (**c**) the probability density function of κ_{gf} ~~(κ-PDF)~~ for 40–nm

带格式的: 字体颜色: 文字 1
带格式的: 字体颜色: 文字 1
带格式的: 字体颜色: 文字 1
带格式的: 字体颜色: 文字 1
带格式的: 字体颜色: 文字 1
带格式的: 字体颜色: 文字 1
带格式的: 字体颜色: 文字 1
带格式的: 字体颜色: 文字 1
带格式的: 字体颜色: 文字 1
带格式的: 字体颜色: 文字 1
带格式的: 字体颜色: 文字 1
带格式的: 字体颜色: 文字 1
带格式的: 字体颜色: 文字 1
带格式的: 字体颜色: 文字 1
带格式的: 字体颜色: 文字 1

and (**d**) 150–nm particles from 6 May to 15 June of 2016.

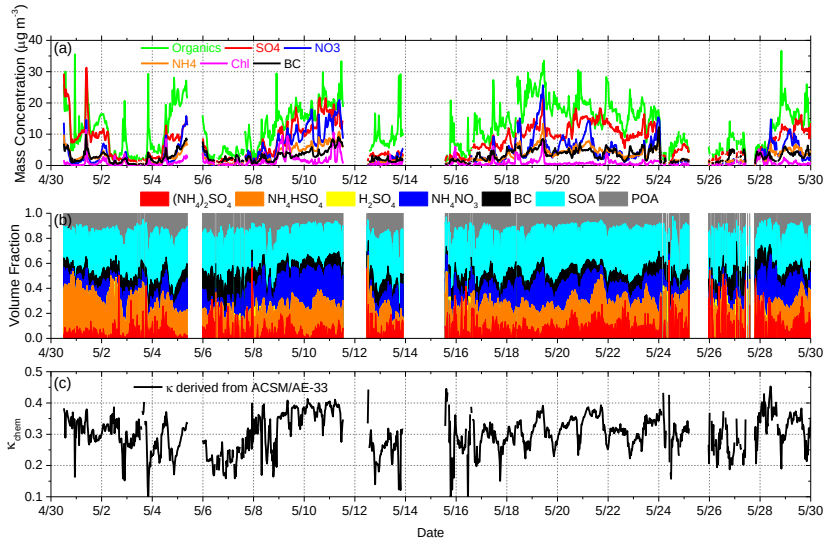

Figure 5. Time series of (**a**) the bulk mass concentration of aerosol species in PM_1, (**b**) the volume fractions of POA, SOA, BC, and inorganics with the simplified ion-pairing scheme, and (**c**) the hygroscopicity parameter derived from the chemical compositions (κ_{chem}).

带格式的: 字体颜色: 文字 1

带格式的: 字体颜色: 文字 1

带格式的: 字体颜色: 文字 1

带格式的: 字体颜色: 文字 1

带格式的: 字体颜色: 文字 1

带格式的: 字体颜色: 文字 1

带格式的: 字体颜色: 文字 1

带格式的: 字体颜色: 文字 1

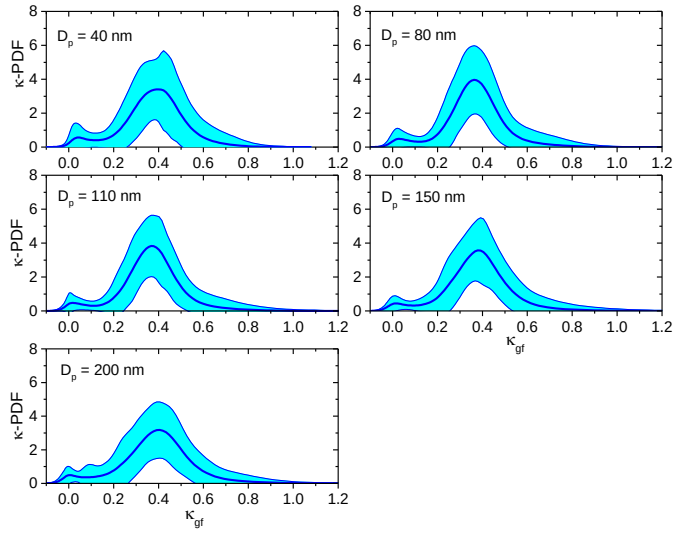

Figure 6. Mean probability density functions of κ_{gf} (κ-PDF) for different particle sizes and their standard deviations (shaded areas) derived from H-TDMA data and measured at RH = 85 %.

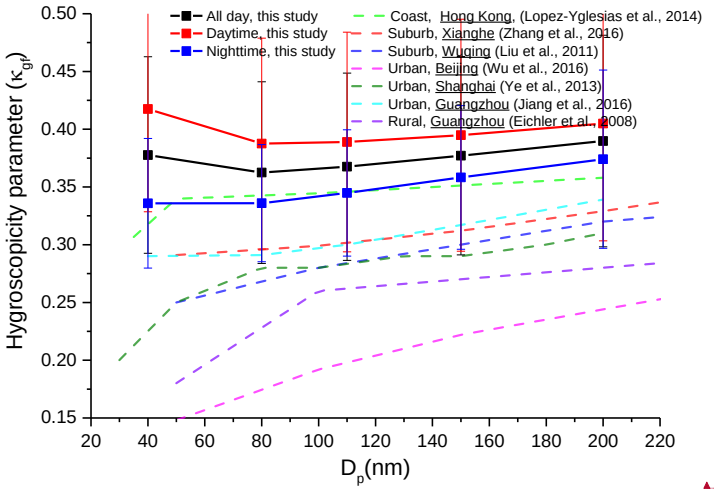

Figure 7. Size-resolved aerosol hygroscopicity parameter (κ_{gf}) derived from H-TDMA data at XT and at other sites in China.

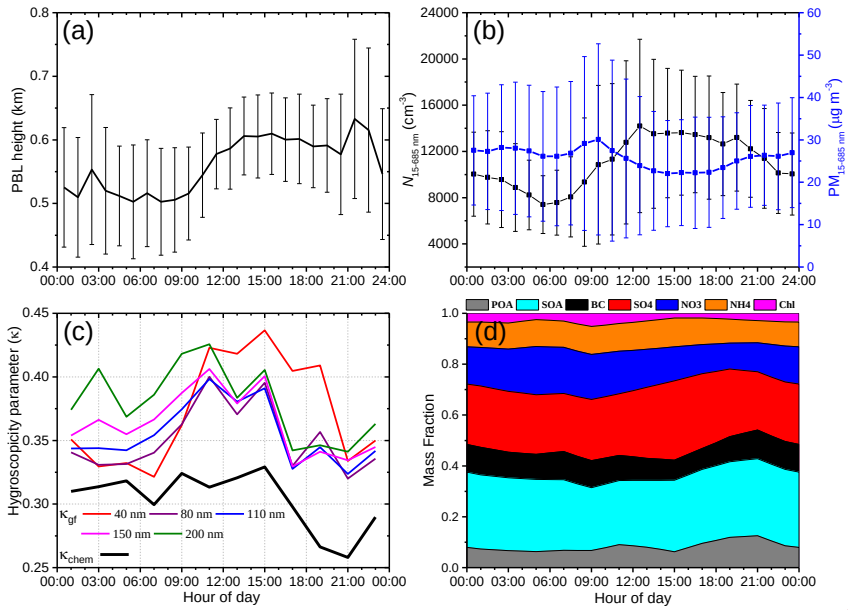

Figure 8. Diurnal variations in (**a**) planetary boundary layer (PBL) height retrieved from ~~the MPL~~micropulse lidar data, (**b**) aerosol number and mass concentrations in the 15–685 nm range ($N_{15–685\ nm}$ and $PM_{15–685\ nm}$, respectively) derived from the SMPS (an aerosol density of 1.6 g cm^{-3} is assumed), (**c**) the hygroscopicity parameter derived from the hygroscopic growth factor (κ_{gf}) and predicted from the bulk chemical composition (κ_{chem}), and (**d**) the mass fractions of different species.

带格式的: 字体颜色: 文字 1
带格式的: 字体颜色: 文字 1
带格式的: 字体颜色: 文字 1
带格式的: 字体颜色: 文字 1
带格式的: 字体颜色: 文字 1
带格式的: 字体颜色: 文字 1
带格式的: 字体颜色: 文字 1
带格式的: 字体颜色: 文字 1
带格式的: 字体颜色: 文字 1

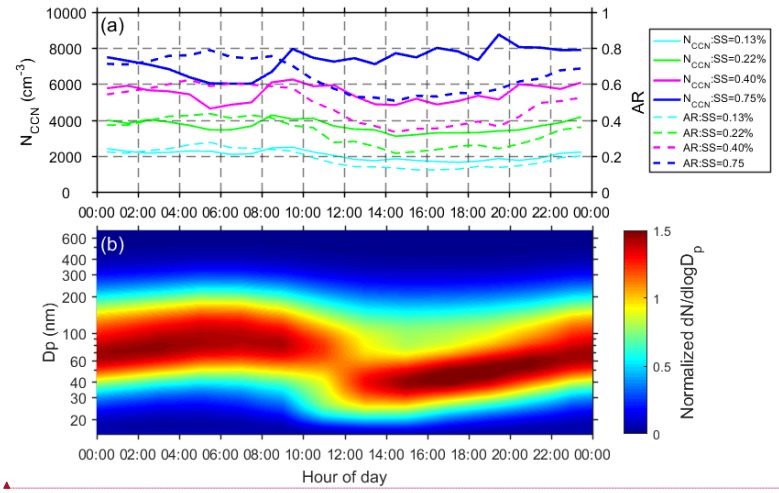

Figure 9. Diurnal variations in (a) CCN number concentration (N_{CCN}) and activation ratio (AR), and (b) the normalized aerosol size distribution in the 15–685 nm particle size range.

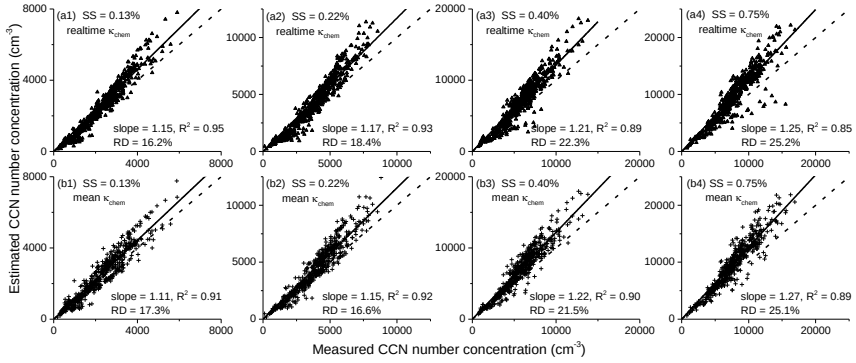

Figure 10. Estimated versus measured cloud condensation nuclei (CCN) number concentrations (N_{CCN}) for ambient aerosols at four different supersaturation (SS) levels. The N_{CCN} is estimated based on κ-Köhler theory~~,~~ using the real-time κ_{chem} (**a1-a4**) and the mean κ_{chem} (**b1-b4**). The slope and ~~correlation~~ coefficient of

determination (R^2) of the linear regression, and the relative deviation (RD) of estimated N_{CCN} (RD = $|N_{CCN\_estimated} - N_{CCN\_measured}| / N_{CCN\_measured}$) are shown in each panel. The regression line is overlaid on the measurements (solid line) and the dashed line is the 1:1 line.

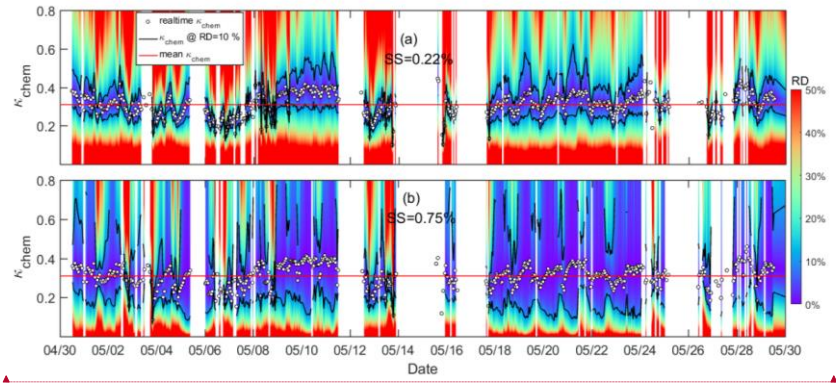

Figure 11. Sensitivity of N_{CCN} estimates to κ_{chem} as a function of time at (a) SS = 0.22-% and (b) SS = 0.75-%. The color scale indicates the relative deviation (RD) of the CCN estimates using the κ_{chem} value shown on the ordinate. In each panel, open circles show the real-time κ_{chem}. Note that RD is by definition zero at these points. The black line is κ at RD = 10-% and the red line is the mean value for κ_{chem} (0.31). Figure S8 in the supplement shows the same plots but for SS = 0.13-% and 0.40-%.

带格式的: 字体颜色: 文字 1
带格式的: 字体颜色: 文字 1
带格式的: 字体颜色: 文字 1
带格式的: 字体颜色: 文字 1
带格式的: 字体颜色: 文字 1
带格式的: 字体颜色: 文字 1
带格式的: 字体颜色: 文字 1
带格式的: 字体颜色: 文字 1
带格式的: 字体颜色: 文字 1
带格式的: 字体颜色: 文字 1
带格式的: 字体颜色: 文字 1
带格式的: 字体颜色: 文字 1
带格式的: 字体颜色: 文字 1
带格式的: 字体颜色: 文字 1
带格式的: 字体颜色: 文字 1
带格式的: 字体颜色: 文字 1